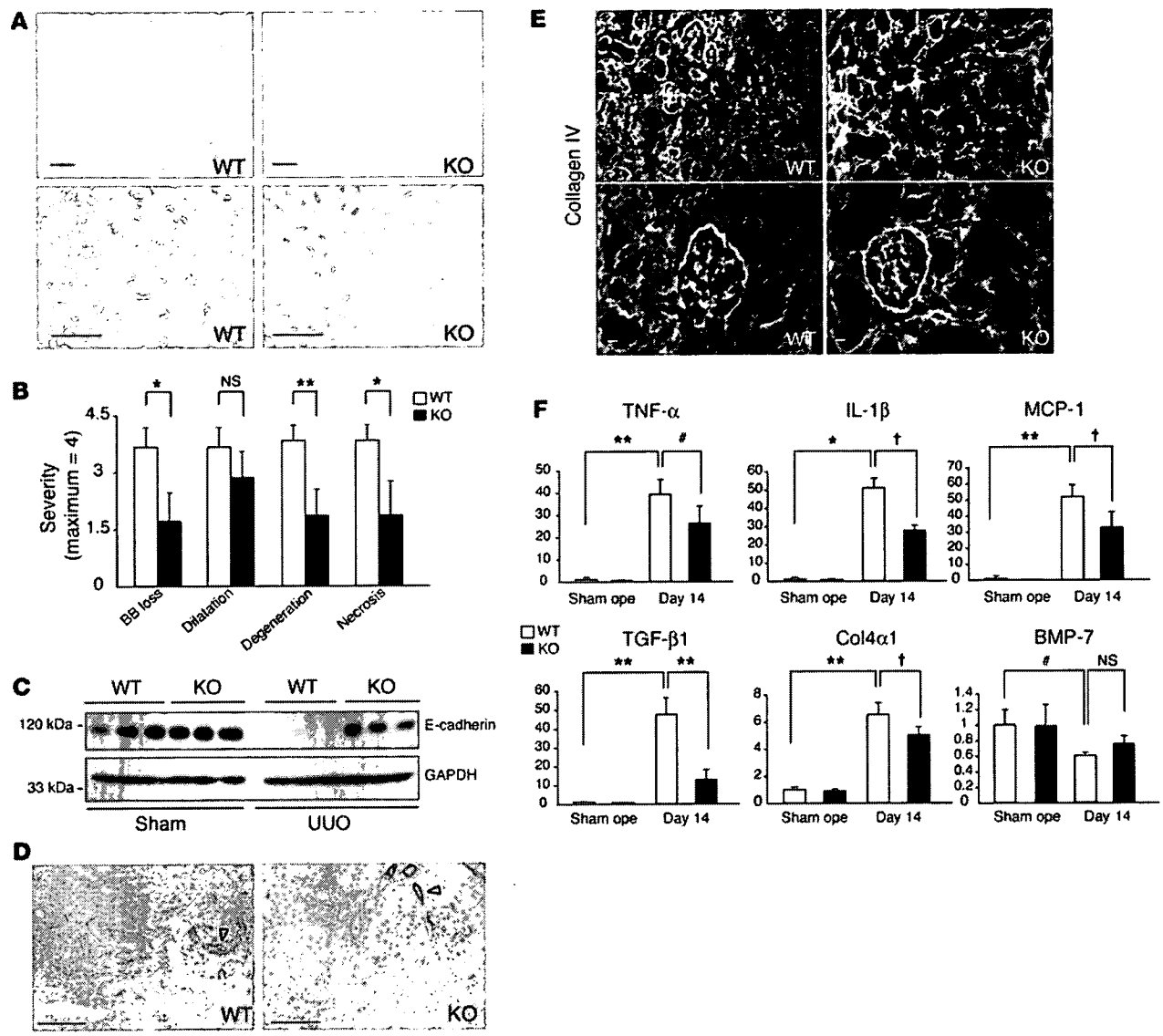

Figure 3

USAG1$^{-/-}$ mice showed reduced EMT and tubulointerstitial fibrosis in UUO. (**A**) Representative histology of the obstructed kidney in wild-type mice and *USAG1*$^{-/-}$ mice 14 days after the operation. Scale bars: 100 μm. (**B**) Semiquantitative evaluation of morphologic kidney damage in wild-type mice and *USAG1*$^{-/-}$ mice, expressed as relative severity on a scale from 0 to 4 (n = 6). (**C**) E-cadherin expression in UUO. Kidney lysates were subjected to immunoblotting with anti–E-cadherin antibody. Representative data from 4 independent experiments are shown. (**D**) Immunostaining of α-SMA in UUO. Arrowheads indicate vascular smooth muscle cells. (**E**) Immunostaining of type IV collagen in UUO. Scale bars: 10 μm. (**F**) Gene expression in UUO. Gene expression was determined by real-time RT-PCR. In each experiment, the expression levels were normalized to the expression of GAPDH and expressed relative to expression in mice on day 0. n = 4–6 for each experiment. $^{\#}P < 0.01$; $^{\dagger}P < 0.005$; $^{*}P < 0.001$; $^{**}P < 0.0001$. Sham ope, mice 14 days after sham operation; day 14, mice 14 days after UUO.

specificity of the antibody against phospho-Smad1/5/8. We also examined the phosphorylation of Smad1/5/8 in immunoblotting of kidney lysates and demonstrated that the phosphorylation was preserved in the kidneys of *USAG1*$^{-/-}$ mice, while it was downregulated in WT mice (Figure 4C). No difference was observed in the phosphorylation of Smad1/5/8 prior to disease induction between *USAG1*$^{-/-}$ mice and WT mice (Figure 4, A and C).

Blocking BMP-7 activity abolishes renoprotection in USAG1$^{-/-}$*mice.* To analyze the mechanism of renoprotection in *USAG1*$^{-/-}$ mice, we administered a neutralizing antibody against BMP-7 to *USAG1*$^{-/-}$ mice in both kidney disease models. First we evaluated the specificity of the neutralizing activity of the antibody using an assay measuring alkaline phosphatase activity and phosphorylation of Smad1/5/8 in C2C12 cells induced by BMPs. Addition of the antibody inhibited the alkaline phosphatase activity and phosphorylation of Smad1/5/8 induced by BMP-7, but not by BMP-4 (Figure 5A) or BMP-2 (data not shown), indicating the specificity of the antibody. As a negative control, we used isotype-matched IgG2B. Next we administered a neutralizing antibody against BMP-7 to *USAG1*$^{-/-}$ mice with cisplatin nephrotoxicity. Of 7 mice treated with neutralizing antibody, 2 mice died on day 2 and 1 mouse died on day 3, while none of the mice treated with isotype-matched IgG2B

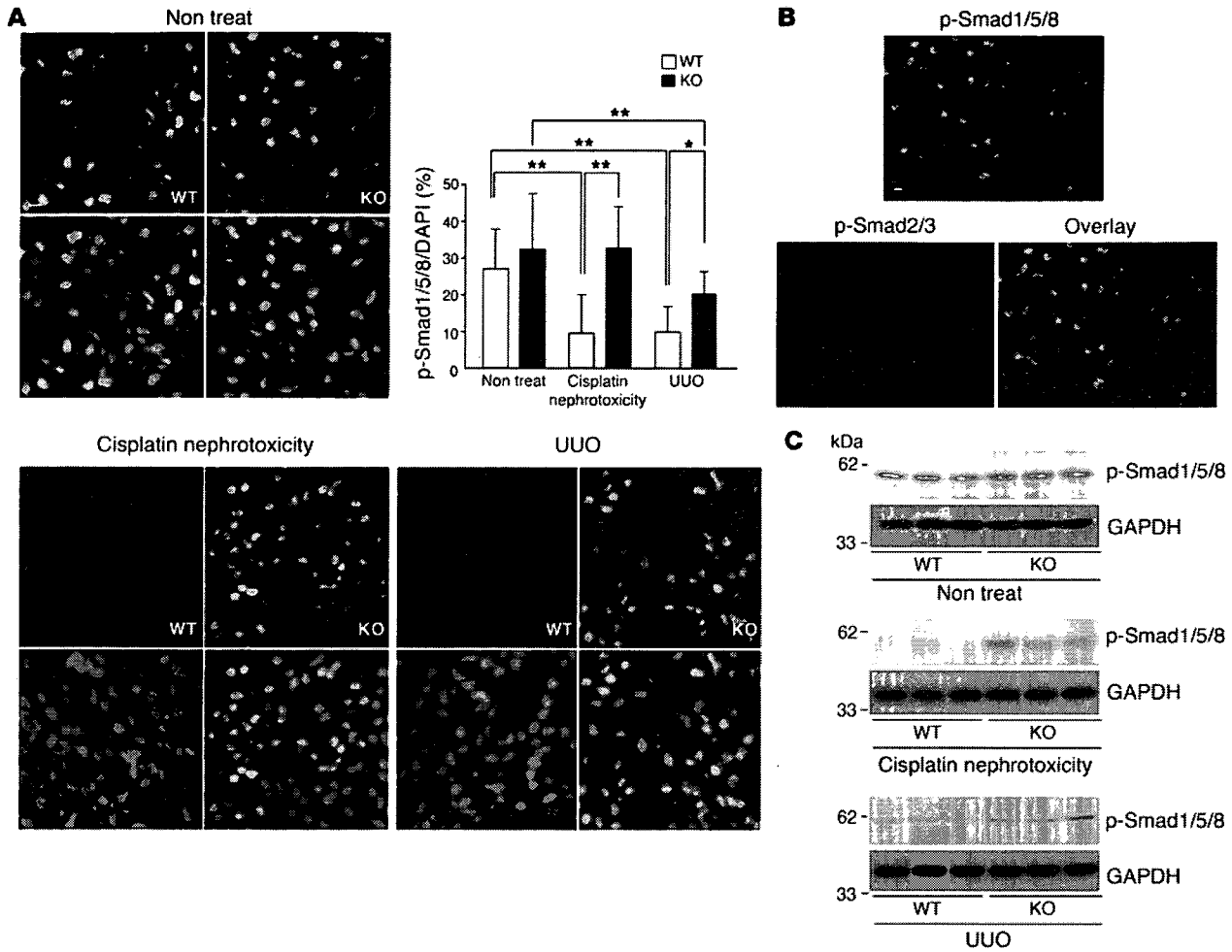

Figure 4
Enhanced BMP signaling in kidneys of *USAG1*$^{-/-}$ mice. (**A**) Phosphorylation of Smad1/5/8 in kidneys of *USAG1*$^{-/-}$ mice and WT mice. The number of pSmad1/5/8-positive nuclei (upper panels) was counted in 10 consecutive fields in each specimen and normalized by the number of DAPI-positive nuclei (lower panels). $n = 6$. Scale bar: 10 μm. $^{*}P < 0.001$; $^{**}P < 0.0001$. Non treat, mice without disease models. (**B**) Double immunostaining of phospho-Smad1/5/8 and phospho-Smad2/3. Almost all the nuclei positive for pSmad1/5/8 were negative for pSmad2/3. Scale bar: 10 μm. (**C**) Immunoblotting of phospho-Smad1/5/8 in kidney lysates prior to disease induction and in both kidney disease models. Representative data from 5 independent experiments are shown.

died within the first 3 days. Administration of neutralizing antibody also resulted in a deterioration of renal function measured by elevation of serum creatinine to a level similar to that in WT mice, while administration of IgG2B did not (Figure 5B). Furthermore, histological examination of the kidneys of *USAG1*$^{-/-}$ mice treated with neutralizing antibody demonstrated severely damaged proximal tubular epithelial cells, while these changes were absent in mice treated with IgG2B (Figure 5B). We also administered the neutralizing antibody to *USAG1*$^{-/-}$ mice with UUO and found that type IV collagen expression in the obstructed kidney was increased in *USAG1*$^{-/-}$ mice treated with neutralizing antibody, but not in those administered IgG2B (Figure 5C). Histological examination of the obstructed kidneys of *USAG1*$^{-/-}$ mice treated with neutralizing antibody demonstrated severe interstitial fibrosis, while this change was almost absent in mice treated with IgG2B (Figure 5C).

USAG1 is the most abundant BMP antagonist in adult kidney. Finally we analyzed the expression of USAG-1 and other BMP antagonists in adult kidneys using modified real-time PCR and in situ hybridization (Figure 6). To compare the expression levels of different genes in real-time PCR, we set the standard curve with the plasmid encoding each BMP antagonist at various concentrations and analyzed the copy number of each gene contained in kidney cDNA. Among known BMP antagonists, USAG-1 was by far the most abundant in the kidneys, and twisted gastrulation was the second most abundant BMP antagonist. We also analyzed the localization of BMP antagonists in the kidneys using in situ hybridization and found that the expression of USAG-1 was confined to distal tubules, as previously described (21), with a pattern similar to that of BMP-7 (12). Expression of twisted gastrulation was also detected in some distal tubules; however, the intensity of the signal was much lower than that of USAG-1, in accordance with the results of real-time PCR. Differential screening-selected gene aberrative in neuroblastoma (DAN) and protein related to DAN and Cerberus (PDRC) were faintly observed in the inner medulla, and other BMP antagonists were not detected with this method.

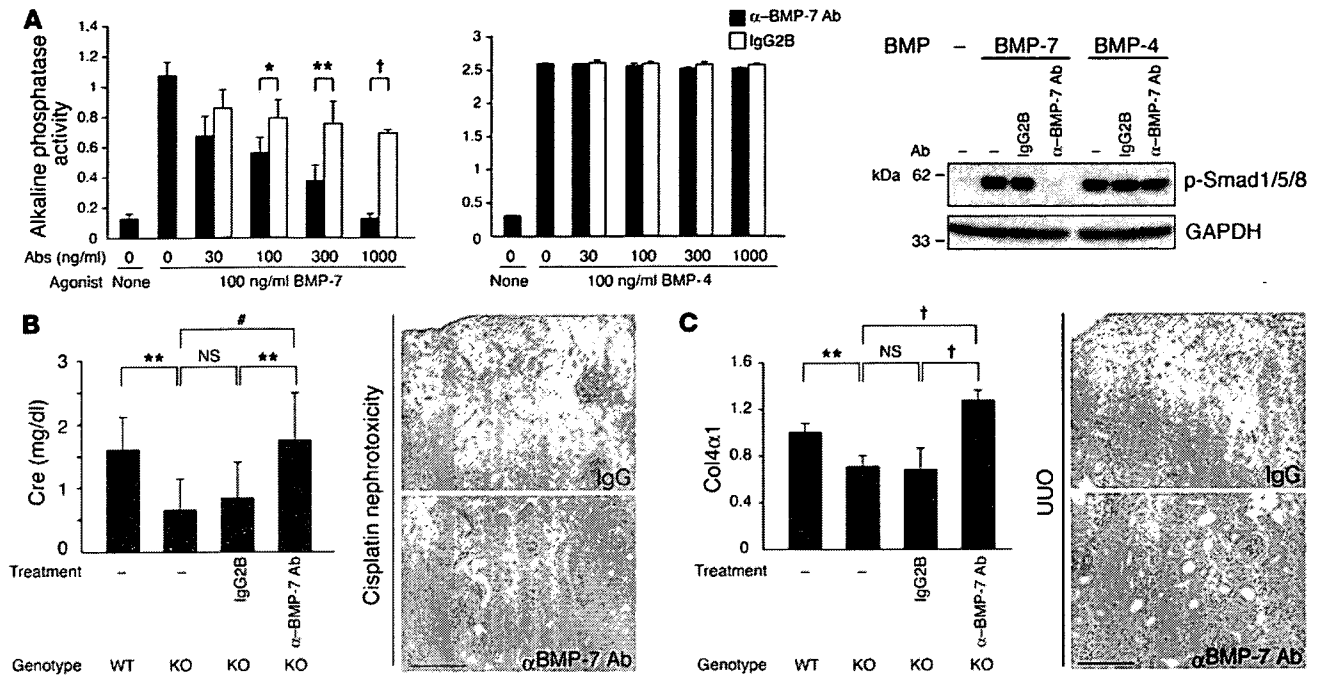

Figure 5

Blocking BMP-7 activity abolishes renoprotection in *USAG1*$^{-/-}$ mice. (**A**) Evaluation of neutralizing activity of anti–BMP-7 antibody. Anti–BMP-7 antibody inhibits alkaline phosphatase activity and phosphorylation of Smad1/5/8 induced by BMP-7, but not by BMP-4. (**B**) Serum creatinine level of *USAG1*$^{-/-}$ mice treated with anti–BMP-7 antibody and representative histological findings on day 3 of cisplatin nephrotoxicity. Scale bar: 100 μm. (**C**) Gene expression of type IV collagen in kidneys of *USAG1*$^{-/-}$ mice treated with anti–BMP-7 antibody and representative histological findings on day 14 of UUO. $^{*}P < 0.1$; $^{**}P < 0.01$; $^{\#}P < 0.001$; $^{\dagger}P < 0.0001$.

Discussion

Epithelial-mesenchymal transition (EMT) is a necessary step for renal fibrosis, as well as in embryonic development and tumor progression (29–31). TGF-β is known to stimulate EMT, while BMP-7 inhibits and reverses the transition (3). Zeisberg et al. recently reported that BMP-7 reverses TGF-β1–induced EMT and induces mesenchymal-epithelial transition in vitro (4, 32). They further demonstrated that administration of a pharmacological dose of BMP-7 resulted in regression of established lesions in the kidney and improved renal function. In this report, we demonstrated that deficiency of USAG-1, a novel BMP antagonist in the kidney, results in marked preservation of renal function by reinforcement of BMP signaling.

Based on these findings, we set the working hypothesis: in many types of renal disease, proximal tubule epithelial cells (PTECs) are the main site of injury (33) and undergo EMT, which causes loss of structural integrity of epithelial cells characterized by a reduction of E-cadherin expression and the induction of α-SMA in interstitial myofibroblasts (Figure 7A). BMP-7 secreted from distal tubules (12) inhibits EMT of PTECs and induces redifferentiation of mesenchymal cells to epithelial cells. USAG-1 produced from distal tubules binds to BMP-7 and inhibits its renoprotective action by interfering with binding to its receptors.

In addition to the inhibition of EMT, many other pharmacological actions of BMP-7 have been reported. Administration of recombinant BMP-7 inhibits the induction of inflammatory cytokine expression in the kidney (12), attenuates inflammatory cell infiltration (6), and reduces apoptosis of tubular epithelial cells in renal disease models (34) (Figure 7A). These phenomena are also observed in *USAG1*$^{-/-}$ mice, and the similarity between BMP-7–treated animals and *USAG1*$^{-/-}$ mice strongly supports our working model that deficiency of USAG-1 reinforces the renoprotective activities of BMP.

In accordance with this hypothesis, the renoprotection in *USAG1*$^{-/-}$ mice was abolished in both renal disease models when a neutralizing antibody against BMP-7 was administered (Figure 5). These results strongly support the hypothesis, and BMP-7 is a potent candidate for the counterpart of USAG-1.

We also observed preserved phosphorylation of Smad1/5/8 in the kidneys of *USAG1*$^{-/-}$ mice in both renal disease models, suggesting that BMP signaling was enhanced in *USAG1*$^{-/-}$ mice, while no difference was observed between WT and KO mice in phosphorylation of Smad1/5/8 prior to disease induction (Figure 4, A and C). We assume that BMP signaling prior to disease induction might be potent enough to cause full phosphorylation of Smad1/5/8 regardless of the presence or absence of USAG-1, while in the later stages of kidney diseases, BMP signaling is decreased and the presence of USAG-1 might cause a further reduction in BMP signaling.

Furthermore, we demonstrated that USAG-1 is by far the most abundant BMP antagonist in the kidney (Figure 6A). Because other BMP antagonists also antagonize BMP-7 activities (Supplemental Figure 2), we conclude that USAG-1 plays an important role in the modulation of BMP activities in the kidney not because of its ligand specificity, but because of its high expression among other BMP antagonists. In addition, the tissue localization of USAG-1 (Figure 6B) is quite similar to that of BMP-7 (12), and USAG-1 can effectively access and inactivate BMP-7 at the site of production.

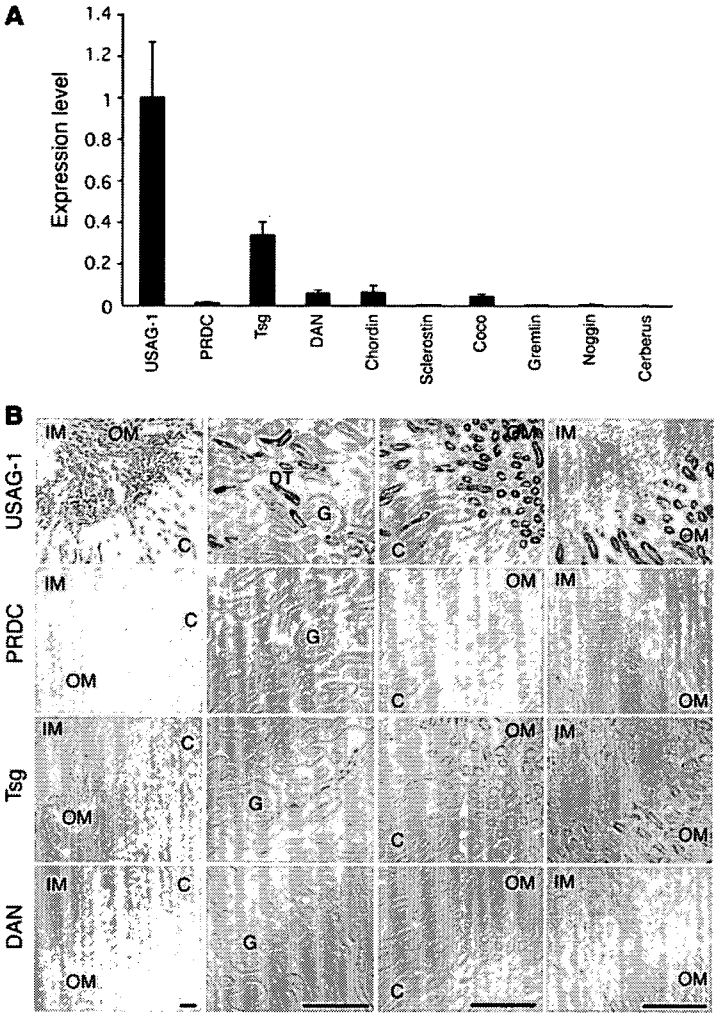

Figure 6
Expression of BMP antagonists in kidney. (**A**) Kidney cDNA of wild-type mice with Svj background was subjected to real-time PCR with various primers for BMP antagonists, and the standard curve was set using the plasmid encoding each BMP antagonist from concentrations of 1 pg/μl to 1 fg/μl. The values of each BMP antagonist in the kidney cDNA were multiplied by the length of the vectors and normalized to the value of USAG-1 expression (n = 4–5). Expression of USAG-1 was by far the most abundant in the kidney among other BMP antagonists. Tsg, twisted gastrulation. (**B**) Kidney sections were subjected to in situ hybridization with probes for all BMP antagonists. Expression of USAG-1 was confined to the distal tubular epithelial cells. Twisted gastrulation was also sparsely expressed in some distal tubules. Differential screening–selected gene aberrative in neuroblastoma (DAN) and protein related to DAN and Cerberus (PDRC) were faintly detected in the inner medulla. Expression of other BMP antagonists was not detected by this method. Scale bars: 100 μm. IM, inner medulla; OM, outer medulla; C, cortex; DT, distal tubule; G, glomerulus.

Although we illustrated USAG-1/BMP-7 binding as occurring outside of PTECs in Figure 7A, it might be possible that the binding occurs intracellularly within the secretory pathway in PTECs and that USAG-1 and BMP-7 are secreted in complex form. Further investigations are necessary to clarify this point.

Interestingly, the expression of USAG-1 decreased during the course of disease models (Supplemental Figure 3 and unpublished observations). We assume that the reduction of USAG-1 in renal diseases is a self-defense mechanism to minimize its inhibitory effect on BMP signaling. Because the reduction in USAG-1 expression in WT mice is not enough to overcome the reduction in BMP-7 expression, further reduction or abolishment of the action of USAG-1 is desirable for the preservation of renal function, and the results of the present study justify therapy targeted toward USAG-1. For example, drugs or neutralizing antibodies that inhibit binding between USAG-1 and BMP or gene-silencing therapy for *USAG1* would enhance the activity of endogenous BMP and might be a promising way to develop novel therapeutic methods for severe renal disease (Figure 7B). Because the expression of USAG-1 is confined to the kidney in adult mice and humans (21), it would be a better target for kidney-specific therapeutic trials. On the other hand, administration of recombinant BMP-7, whose target cells are widely distributed throughout the body, might produce some additional extrarenal actions, including beneficial effects, such as actions on renal osteodystrophy (35–39) and vascular calcification (40, 41).

Furthermore, these therapies targeted toward USAG-1 might protect the kidney during administration of nephrotoxic agents such as cisplatin. The pathological roles of USAG-1 in glomerular injury should be further elucidated before we undertake therapeutic trials against USAG-1.

Despite the essential role of BMP-7 in renal development, we did not observe any developmental abnormality in the kidney of *USAG1*$^{-/-}$ mice with this genetic background. We assume that there are many reasons for the lack of developmental abnormality: First, USAG-1 expression in the developing kidney is not apparent on embryonic day 11.5 (21), whereas BMP-7 expression is intense in the metanephric mesenchyme (42) with a pattern similar to that of gremlin (43). In the later stages, USAG-1 expression appears in the tubular epithelium in the medullary region (21), whereas BMP-7 expression is confined to the condensed mesenchyme and peripheral ureteric epithelium (42). Therefore, the expression pattern of USAG-1 in the developing kidney is totally different from that of BMP-7. Second, the expression of USAG-1 is very low in early embryogenesis, increases toward the late stage of embryogenesis, and is much higher in the adult kidney (21), while the expression of gremlin is high in early embryogenesis with a pattern similar to that of BMP-7, and becomes almost undetectable in the healthy adult kidney (Figure 6). Furthermore, *gremlin*-deficient mice show severe developmental abnormality in the kidney, which is quite similar to that of *BMP-7*-deficient mice. Therefore, we conclude that gremlin is a regulator of BMP-7 activity in the developing kidney, and lack of USAG-1 might be compensated by gremlin and does not cause any developmental abnormality in the kidney.

Recently another function of USAG-1 as a modulator of Wnt signaling has been reported in *Xenopus* embryogenesis (44). Although the role of the Wnt pathway in the progression of renal diseases remains to be elucidated, there is a possibility that modulation of the Wnt pathway might also play some roles in the preservation of renal function in *USAG1*$^{-/-}$ mice. Close relationships between the Wnt and BMP pathways have also been reported; for instance, dickkopf homolog 1 (DKK1), a Wnt antagonist, and noggin, a BMP antagonist, cooperate in head induction, while the expression of

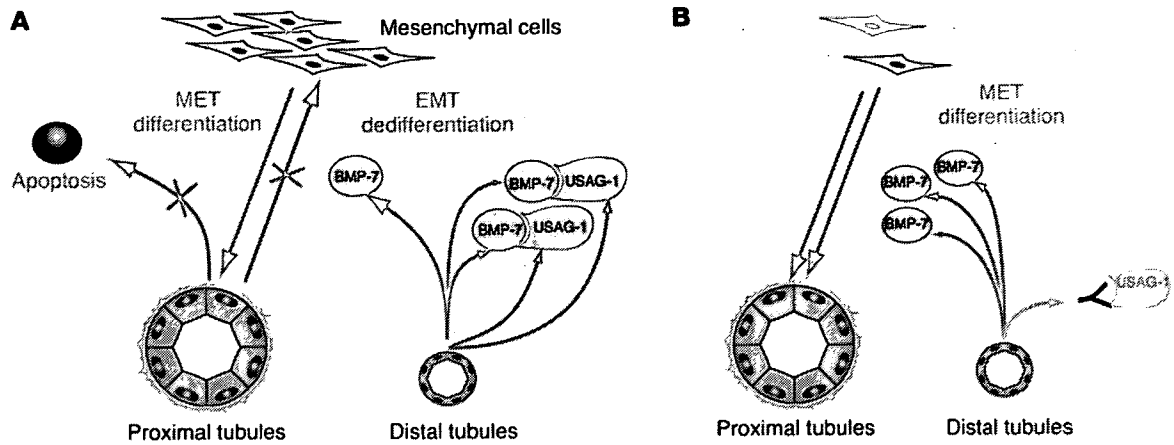

Figure 7
Working model of role of BMP-7 and USAG-1 in renal diseases. (**A**) In renal injury, PTECs are mainly damaged and undergo EMT to fibroblast-like mesenchymal cells. BMP-7 secreted by the distal tubule inhibits EMT and apoptosis of PTECs. USAG-1 is also secreted by the distal tubule, binds to BMP-7, and inhibits the renoprotective actions of BMP-7. (**B**) Therapeutic implication of USAG-1. Reduction of USAG-1 activity, for example, by a neutralizing antibody blocking the binding of USAG-1 and BMP-7, results in reinforcement of the renoprotective action of BMP-7. MET, mesenchymal-epithelial transition.

DKK1 is regulated by BMP-4 in limb development. Furthermore, a BMP antagonist, cerberus, has binding sites for both Wnt and BMP and antagonizes the activities of both the Wnt and BMP signaling pathways. USAG-1 might also have dual activities and act as a molecular link between these 2 important signaling pathways.

In conclusion, this study showed that USAG-1 plays important roles in the progression of renal diseases and might be a potent negative regulator of the renoprotective action of endogenous BMP signaling. Recently, Lin et al. identified a positive regulator of BMP-7 named kielin/chordin-like protein (KCP) and demonstrated that *KCP*$^{-/-}$ mice are susceptible to tubular injury and interstitial fibrosis (45). These data support the idea that BMP-7 protects the kidney from renal injury. Because these negative and positive modulators of BMP signaling regulate and edge the boundaries of BMP activity, further understanding of these modulators would give valuable information about their pathophysiological functions and provide a rationale for a therapeutic approach against these proteins.

Methods

Generation of USAG1$^{-/-}$ *mice.* We isolated a genomic fragment containing the mouse *USAG1* gene by screening a 129/SvJ genomic library (Stratagene). We inserted an *nlacZ* gene and a PGK-*Neo*R cassette in the opposite transcriptional orientation to the *USAG1* gene. ES cells were transfected with the linearized targeting vector by electroporation and selected by G418-containing medium. Homologous recombinants were screened and identified by genomic Southern blot analysis with an *Hin*cII-*Eco*RI probe mapping outside the 5′ homology arm (Figure 1A). Homologous recombined ES cell clones were obtained, and correct recombination was confirmed by Southern blot (Figure 1B) as well as PCR analyses. ES cells carrying the *USAG1*-null allele were injected into C57BL/6 blastocysts to obtain chimeric mice, which were crossed with wild-type C57BL/6J mice. Following germline transmission, the mice were maintained in a mixed SvJ background. PCR genotyping was used for all subsequent studies to allow specific detection of both the wild-type and *USAG1*$^{-/-}$ alleles (Figure 1C). Sequences of the primers used for genotyping are as follows: F1, CCCCTCCTCATCTGGCTGCTTCCTAAACGG; R1, CAGTCACGACGTTGTAAAACGACGGGATCC; F2, GGGATCCCACCCCTTCTCT; and R2, GCCGGGACAGGTTTAACCA.

Animal use. All experiments except those represented in Supplemental Figure 3 were performed using *USAG1*$^{-/-}$ mice and their wild-type littermates (*USAG1*$^{+/+}$) of the F_2 generation. All mice were housed in specific pathogen-

Table 1
Primers for real-time RT-PCR

Gene	Sequence of primers (5′-3′)
GAPDH	CCAGAACATCATCCCTGCATC; CCTGCTTCACCACCTTCTTGA
TNFα	ATGAGAAGTTCCCAAATGGCC; CCTCCACTTGGTGGTTTGCTA
IL-1β	CCTTCCAGGATGAGGACATGA; AACGTCACACACCAGCAGGTT
TGFβ1	GCAACAATTCCTGGCGTTACC; CGAAAGCCCTGTATTCCGTCT
MCP-1	TGCATCTGCCCTAAGGTCTTC; AAGTGCTTGAGGTGGTTGTGG
Col4α1	TTCCTTCGTGATGCACACCA; TTCTCATGCACACTTGGCAGC
USAG1	GCAACAGCACCCTGAATCAAG; TGTATTTGGTGGACCGCAGTT
Chordin	GCAGTGGTTCCCAGAGAATCA; AACAATCGTCCCGCTCACAGT
DAN	CTTCAGTTACAGCGTCCCCAA; CCAAGGTCACAATCTCCCACA
PRDC	AGGAGGCTTCCATCTCGTCAT; CCGGTTCTTCCGTGTTTCA
Twisted gastrulation	AAACGTGTCTGTTCCCAGCAA; ACACTGGTGGATGGACATGCA
Gremlin	AGCCCAAGAAGTTCACCACCA; TATGCAACGGCACTGCTTCAC
Sclerostin	CAAGCCTTCAGGAATGATGCC; TCGGACACATCTTTGGCGT
Noggin	AGAAACAGCGCCTGAGCAAGA; AAAAGCGGCTGCCTAGGTCAT
Cerberus	CCCATCAAAAGCCACGAAGT; CCAAAGCAAAGGTTGTTCTGG
Coco	TCCGCTTTTAGCCACTAGGTG; GCTGTTATTCTGGTGTCCCCA
BMP-2	TCGACCATGGTGGCCGGGACCCG; TGTTCCCGGAAGATCTGGAGT
BMP-3	AGCGAATGGATTATCTCTCCCA; TCTTTTCCGGCACACAGCA
BMP-4	CTGGAATGATTGGATTGTGGC; GCATGGTTGGTTGAGTTGAGG
BMP-5	AAGCCTGCAAGAAGCACGAA; GGAAAAGAACATTCCCCGTCA
BMP-6	CCAACCACGCCATTGTACAGA; GGAATCCAAGGCAGAACCATG
BMP-7	TGTGGCAGAAAACAGCAGCA; TCAGGTGCAATGATCCAGTCC

free conditions. Experiments represented in Supplemental Figure 3 were performed using C57BL/6 mice. All animal experiments were approved by the Animal Research Committee at the Graduate School of Medicine, Kyoto University, and the Animal Experiment and Use Committee at the University of Tsukuba and were in accordance with NIH guidelines.

Cisplatin administration. Cisplatin (Sigma-Aldrich) was administered at 20 mg/kg to mice by a single intraperitoneal injection. Mice were sacrificed 72 hours after administration of cisplatin, and tissue and blood were collected for further analysis.

UUO. Complete UUO was performed as previously described (46). Briefly, under sodium pentobarbital anesthesia, the middle portion of the left ureter was ligated and cut between 2 ligated points. At 14 days after surgery, the mice were sacrificed, and the obstructed kidneys were subjected to the studies described below.

Histological studies. The kidneys were fixed in Carnoy solution and embedded in paraffin. Sections (2 μm) were stained with PAS for routine histological examination, and the degree of morphological changes was determined using light microscopy. The following parameters were chosen as indicative of morphological damage to the kidney after cisplatin injection and UUO: brush border loss, tubule dilatation, tubule degeneration, and tubule necrosis. These parameters were evaluated on a scale of 0 to 4, and classed as: 0, not present; 1, mild; 2, moderate; 3, severe; and 4, very severe. The remaining kidney was used for immunohistochemical study, RNA isolation, and protein extraction.

Immunostaining. Frozen sections of kidneys were subjected to immunostaining with polyclonal antibodies against type IV collagen (ICN Pharmaceuticals), phosphorylated Smad1/5/8 (Cell Signaling Technology), and phosphorylated Smad2/3 (Santa Cruz Biotechnology Inc.) and monoclonal antibodies against α-SMA (Sigma-Aldrich) and Mac-1 (BD Biosciences – Pharmingen) as previously described (47, 48).

Immunoblotting. Whole kidney protein was homogenized in RIPA buffer (50 mM Tris at pH 7.5, 150 mM NaCl, 1% Nonidet P-40, 0.25% SDS, 1 mM Na_3VO_4, 2 mM EDTA, 1 mM PMSF, and 10 μg/ml aprotinin) and subjected to immunoblotting as described previously (49). Anti-E-cadherin antibody and anti-GAPDH antibody were from BD Biosciences – Transduction Laboratories and Research Diagnostic Inc., respectively.

Apoptosis detection and quantification. The TUNEL technique (In Situ Cell Death Detection Kit; Roche Diagnostics GmbH) was used to detect apoptotic cells in situ. All apoptotic nuclei within a transverse section at the renal pelvis were counted.

Quantification of mRNA by real-time RT-PCR. Real-time RT-PCR was performed with a 7700 Sequence Detection System (Applied Biosystems). Five micrograms of total RNA was reverse transcribed in a reaction volume of 20 μl using Superscript III reverse transcriptase and random primers (Invitrogen Corp.). The product was diluted to a volume of 400 μl, and 5-μl aliquots were used as templates for amplification using SYBR Green PCR amplification reagent (Applied Biosystems) and gene-specific primers. Specific primers for each gene transcript (listed in Table 1) were designed using Primer Express software version 2.0.0 (Applied Biosystems) and checked as to whether they showed a single peak in the dissociation curve. Serially diluted cDNA or plasmids encoding probes for in situ hybridization were used to generate the standard curve for each primer, and the PCR conditions were as follows: 50°C for 2 minutes, 95°C for 10 minutes, then 95°C for 15 seconds and 60°C for 1 minute for 40 cycles.

Administration of neutralizing antibody against BMP-7. In cisplatin nephrotoxicity, 1.5 mg/kg neutralizing anti-BMP-7 antibody (R&D Systems Inc.) was peritoneally injected into *USAG1*$^{-/-}$ mice 24 hours after injection of cisplatin. In UUO, 0.5 mg/kg neutralizing anti-BMP-7 antibody was injected every 3 days from day 2 to day 11. As a negative control, isotype-matched IgG2B (BD Biosciences) was injected at the same time points. Neutralizing activity of the antibody was evaluated by an assay measuring the production of alkaline phosphatase activity by C2C12 cells, as previously described (21).

In situ hybridization. The kidneys were excised from adult male mice and fixed in 4% paraformaldehyde in PBS. Frozen sections (5 μm thick) were treated with 1 μg/ml proteinase K in PBS at 37°C for 30 minutes and acetylated in 0.1 M triethanolamine-HCl, 0.25% acetic anhydride for 15 minutes. Hybridization was performed with probes at concentrations of about 1 μg/ml in a hybridization solution (50% formamide, ×5 SSC, 1% SDS, 50 μg/ml transfer RNA, and 50 μg/ml heparin) at 60°C for 16 hours. RNA probes were synthesized by in vitro transcription with a DIG RNA Labeling Mix (Roche Diagnostics Corp.). Each probe was designed to contain an open reading frame with the following length and G+C content: USAG-1, 1.0 kbp (G+C 52.6%); sclerostin, 1.5 kbp (61.7%); coco, 1.2 kbp (54.7%); DAN, 1.0 kbp (60.6%); twisted gastrulation, 0.7 kbp (55.1%); PRDC, 0.8 kbp (57.7%); chordin, 1.5 kbp (60.2%); gremlin, 0.9 kbp (50%); noggin, 0.7 kbp (64.7%); cerberus, 1.5 kbp (48.8%). Hybridization was detected using an anti-DIG AP conjugate (Roche Diagnostic Corp.) and NBT/BCIP solution (Roche Diagnostics Corp.).

Analysis of phenotype of adult teeth. Skeletal preparations of the maxillae and mandibles were made by soaking the mouse heads in 0.02% proteinase K in PBS at 37°C for 4 days after peeling off the skin, dissecting the maxillae and mandibles, and clearing them in 5% H_2O_2 at room temperature for 5 minutes. Finally they were rinsed in H_2O and left to dry.

Statistics. All assays were performed in triplicate. Data are presented as mean ± SD. Statistical significance was assessed by ANOVA, followed by Fisher's protected least significant difference post-hoc test. Survival curves were derived using the Kaplan-Meier method and compared using log-rank test.

Acknowledgments

We are grateful to Y. Nabeshima, T. Nakahata, and T. Nakamura for helpful discussion. We are grateful to M. Yoshimoto for hematological evaluation of the mice. We thank A. Godo, H. Uchiyama, and A. Hosoya for technical assistance. We thank W. Gray for reading the manuscript.

Received for publication April 25, 2005, and accepted in revised form October 11, 2005.

Address correspondence to: Motoko Yanagita, COE Formation for Genomic Analysis of Disease Model Animals with Multiple Genetic Alterations, Graduate School of Medicine, Kyoto University, Shogoin Kawahara-cho 54, Kyoto 606-8507, Japan. Phone: 81-75-751-3465; Fax: 81-75-751-3574; E-mail: motoy@kuhp.kyoto-u.ac.jp.

1. Eddy, A.A. 1996. Molecular insights into renal interstitial fibrosis. *J. Am. Soc. Nephrol.* **7**:2495–2508.
2. van Kooten, C., Daha, M.R., and van Es, L.A. 1999. Tubular epithelial cells: a critical cell type in the regulation of renal inflammatory processes. *Exp. Nephrol.* **7**:429–437.
3. Neilson, E.G. 2005. Setting a trap for tissue fibrosis. *Nat. Med.* **11**:373–374.
4. Zeisberg, M., et al. 2003. BMP-7 counteracts TGF-beta1-induced epithelial-to-mesenchymal transition and reverses chronic renal injury. *Nat. Med.* **9**:964–968.
5. Vukicevic, S., et al. 1998. Osteogenic protein-1 (bone morphogenetic protein-7) reduces severity of injury after ischemic acute renal failure in rat. *J. Clin. Invest.* **102**:202–214.
6. Hruska, K.A., et al. 2000. Osteogenic protein-1 prevents renal fibrogenesis associated with ureteral obstruction. *Am. J. Physiol. Renal. Physiol.* **279**:F130–F143.
7. Hruska, K.A. 2002. Treatment of chronic tubulointerstitial disease: a new concept. *Kidney Int.* **61**:1911–1922.
8. Zeisberg, M., et al. 2003. Bone morphogenic protein-7 inhibits progression of chronic renal fibrosis associated with two genetic mouse models. *Am. J. Physiol. Renal. Physiol.* **285**:F1060–F1067.

9. Dudley, A.T., Lyons, K.M., and Robertson, E.J. 1995. A requirement for bone morphogenetic protein-7 during development of the mammalian kidney and eye. *Genes Dev.* **9**:2795–2807.
10. Luo, G., et al. 1995. BMP-7 is an inducer of nephrogenesis, and is also required for eye development and skeletal patterning. *Genes Dev.* **9**:2808–2820.
11. Ozkaynak, E., et al. 1990. OP-1 cDNA encodes an osteogenic protein in the TGF-beta family. *EMBO J.* **9**:2085–2093.
12. Gould, S.E., Day, M., Jones, S.S., and Dorai, H. 2002. BMP-7 regulates chemokine, cytokine, and hemodynamic gene expression in proximal tubule cells. *Kidney Int.* **61**:51–60.
13. Simon, M., et al. 1999. Expression of bone morphogenetic protein-7 mRNA in normal and ischemic adult rat kidney. *Am. J. Physiol.* **276**:F382–F389.
14. Wang, S.N., Lapage, J., and Hirschberg, R. 2001. Loss of tubular bone morphogenetic protein-7 in diabetic nephropathy. *J. Am. Soc. Nephrol.* **12**:2392–2399.
15. Lund, R.J., Davies, M.R., and Hruska, K.A. 2002. Bone morphogenetic protein-7: an anti-fibrotic morphogenetic protein with therapeutic importance in renal disease. *Curr. Opin. Nephrol. Hypertens.* **11**:31–36.
16. Almanzar, M.M., et al. 1998. Osteogenic protein-1 mRNA expression is selectively modulated after acute ischemic renal injury. *J. Am. Soc. Nephrol.* **9**:1456–1463.
17. Massague, J., and Chen, Y.G. 2000. Controlling TGF-beta signaling. *Genes Dev.* **14**:627–644.
18. Simmons, D.G., and Kennedy, T.G. 2002. Uterine sensitization-associated gene-1: a novel gene induced within the rat endometrium at the time of uterine receptivity/sensitization for the decidual cell reaction. *Biol. Reprod.* **67**:1638–1645.
19. Avsian-Kretchmer, O., and Hsueh, A.J. 2004. Comparative genomic analysis of the eight-membered ring cystine knot-containing bone morphogenetic protein antagonists. *Mol. Endocrinol.* **18**:1–12.
20. Laurikkala, J., Kassai, Y., Pakkasjarvi, L., Thesleff, I., and Itoh, N. 2003. Identification of a secreted BMP antagonist, ectodin, integrating BMP, FGF, and SHH signals from the tooth enamel knot. *Dev. Biol.* **264**:91–105.
21. Yanagita, M., et al. 2004. USAG1: a bone morphogenetic protein antagonist abundantly expressed in the kidney. *Biochem. Biophys. Res. Commun.* **316**:490–500.
22. Schrier, R.W. 2002. Cancer therapy and renal injury. *J. Clin. Invest.* **110**:743–745. doi:10.1172/JCI200216568.
23. Megyesi, J., Safirstein, R.L., and Price, P.M. 1998. Induction of p21WAF1/CIP1/SDI1 in kidney tubule cells affects the course of cisplatin-induced acute renal failure. *J. Clin. Invest.* **101**:777–782.
24. Ramesh, G., and Reeves, W.B. 2002. TNF-α mediates chemokine and cytokine expression and renal injury in cisplatin nephrotoxicity. *J. Clin. Invest.* **110**:835–842. doi:10.1172/JCI200215606.
25. Yang, J., and Liu, Y. 2001. Dissection of key events in tubular epithelial to myofibroblast transition and its implications in renal interstitial fibrosis. *Am. J. Pathol.* **159**:1465–1475.
26. Klahr, S., and Morrissey, J. 2002. Obstructive nephropathy and renal fibrosis. *Am. J. Physiol. Renal. Physiol.* **283**:F861–F875.
27. Chevalier, R.L. 1999. Molecular and cellular pathophysiology of obstructive nephropathy. *Pediatr. Nephrol.* **13**:612–619.
28. Sato, M., Muragaki, Y., Saika, S., Roberts, A.B., and Ooshima, A. 2003. Targeted disruption of TGF-beta1/Smad3 signaling protects against renal tubulointerstitial fibrosis induced by unilateral ureteral obstruction. *J. Clin. Invest.* **112**:1486–1494. doi:10.1172/JCI200319270.
29. Kalluri, R., and Neilson, E.G. 2003. Epithelial-mesenchymal transition and its implications for fibrosis. *J. Clin. Invest.* **112**:1776–1784. doi:10.1172/JCI200320530.
30. Bottinger, E.P., and Bitzer, M. 2002. TGF-beta signaling in renal disease. *J. Am. Soc. Nephrol.* **13**:2600–2610.
31. Iwano, M., et al. 2002. Evidence that fibroblasts derive from epithelium during tissue fibrosis. *J. Clin. Invest.* **110**:341–350. doi:10.1172/JCI200215518.
32. Zeisberg, M., Shah, A.A., and Kalluri, R. 2005. Bone morphogenic protein-7 induces mesenchymal to epithelial transition in adult renal fibroblasts and facilitates regeneration of injured kidney. *J. Biol. Chem.* **280**:8094–8100.
33. Gerritsma, J.S., van Kooten, C., Gerritsen, A.F., van Es, L.A., and Daha, M.R. 1998. Transforming growth factor-beta 1 regulates chemokine and complement production by human proximal tubular epithelial cells. *Kidney Int.* **53**:609–616.
34. Li, T., Surendran, K., Zawaideh, M.A., Mathew, S., and Hruska, K.A. 2004. Bone morphogenetic protein 7: a novel treatment for chronic renal and bone disease. *Curr. Opin. Nephrol. Hypertens.* **13**:417–422.
35. Davies, M.R., Lund, R.J., Mathew, S., and Hruska, K.A. 2005. Low turnover osteodystrophy and vascular calcification are amenable to skeletal anabolism in an animal model of chronic kidney disease and the metabolic syndrome. *J. Am. Soc. Nephrol.* **16**:917–928.
36. Gonzalez, E.A., et al. 2002. Treatment of a murine model of high-turnover renal osteodystrophy by exogenous BMP-7. *Kidney Int.* **61**:1322–1331.
37. Hruska, K.A., et al. 2004. Kidney-bone, bone-kidney, and cell-cell communications in renal osteodystrophy. *Semin. Nephrol.* **24**:25–38.
38. Lund, R.J., Davies, M.R., Brown, A.J., and Hruska, K.A. 2004. Successful treatment of an adynamic bone disorder with bone morphogenetic protein-7 in a renal ablation model. *J. Am. Soc. Nephrol.* **15**:359–369.
39. Simic, P., and Vukicevic, S. 2005. Bone morphogenetic proteins in development and homeostasis of kidney. *Cytokine Growth Factor Rev.* **16**:299–308.
40. Davies, M.R., Lund, R.J., and Hruska, K.A. 2003. BMP-7 is an efficacious treatment of vascular calcification in a murine model of atherosclerosis and chronic renal failure. *J. Am. Soc. Nephrol.* **14**:1559–1567.
41. Hruska, K.A., Mathew, S., and Saab, G. 2005. Bone morphogenetic proteins in vascular calcification. *Circ. Res.* **97**:105–114.
42. Godin, R.E., Takaesu, N.T., Robertson, E.J., and Dudley, A.T. 1998. Regulation of BMP7 expression during kidney development. *Development.* **125**:3473–3482.
43. Michos, O., et al. 2004. Gremlin-mediated BMP antagonism induces the epithelial-mesenchymal feedback signaling controlling metanephric kidney and limb organogenesis. *Development.* **131**:3401–3410.
44. Itasaki, N., et al. 2003. Wise, a context-dependent activator and inhibitor of Wnt signalling. *Development.* **130**:4295–4305.
45. Lin, J., et al. 2005. Kielin/chordin-like protein, a novel enhancer of BMP signaling, attenuates renal fibrotic disease. *Nat. Med.* **11**:387–393.
46. Nishida, M., et al. 2002. Absence of angiotensin II type 1 receptor in bone marrow-derived cells is detrimental in the evolution of renal fibrosis. *J. Clin. Invest.* **110**:1859–1868. doi:10.1172/JCI200215045.
47. Yanagita, M., et al. 2001. Gas6 regulates mesangial cell proliferation through Axl in experimental glomerulonephritis. *Am. J. Pathol.* **158**:1423–1432.
48. Yanagita, M., et al. 2001. Gas6 induces mesangial cell proliferation via latent transcription factor STAT3. *J. Biol. Chem.* **276**:42364–42369.
49. Yanagita, M., et al. 2002. Essential role of Gas6 for glomerular injury in nephrotoxic nephritis. *J. Clin. Invest.* **110**:239–246. doi:10.1172/JCI200214861.

Expression of BMP-7 and USAG-1 (a BMP antagonist) in kidney development and injury

M Tanaka[1], S Endo[1], T Okuda[2], AN Economides[3], DM Valenzuela[3], AJ Murphy[3], E Robertson[4], T Sakurai[5], A Fukatsu[6], GD Yancopoulos[3], T Kita[1] and M Yanagita[2]

[1]*Department of Cardiovascular Medicine, Graduate School of Medicine, Kyoto University, Kyoto, Japan;* [2]*COE Formation for Genomic Analysis of Disease Model Animals with Multiple Genetic Alterations, Graduate School of Medicine, Kyoto University, Kyoto, Japan;* [3]*Regeneron Pharmaceuticals Inc., Tarrytown, New York, USA;* [4]*Wellcome Trust Center for Human Genetics, University of Oxford, Oxford, UK;* [5]*Department of Pharmacology, Institute of Basic Medical Sciences, University of Tsukuba, Ibaraki, Japan and* [6]*Department of Artificial Kidneys, Graduate School of Medicine, Kyoto University, Kyoto, Japan*

Once developed, end-stage renal disease cannot be reversed by any current therapy. Bone morphogenetic protein-7 (BMP-7), however, is a possible treatment for reversing end-stage renal disease. Previously, we showed that the BMP antagonist uterine sensitization-associated gene-1 (USAG-1, also known as ectodin and sclerostin domain-containing 1) negatively regulates the renoprotective action of BMP-7. Here, we show that the ratio between USAG-1 and BMP-7 expression increased dramatically in the later stage of kidney development, with USAG-1 expression overlapping BMP-7 only in differentiated distal tubules. Examination of USAG-1 expression in developing kidney indicated that a mosaic of proximal and distal tubule marker-positive cells reside side by side in the immature nephron. This suggests that each cell controls its own fate for becoming a proximal or distal tubule cell. In kidney injury models, the ratio of USAG-1 to BMP-7 expression decreased with kidney damage but increased after subsequent kidney regeneration. Our study suggests that USAG-1 expression in a kidney biopsy could be useful in predicting outcome.

Kidney International (2008) **73**, 181–191; doi:10.1038/sj.ki.5002626; published online 17 October 2007

KEYWORDS: kidney disease; differentiation; nephron segment

Correspondence: *M Yanagita, Graduate School of Medicine, Kyoto University, Yoshida-Konoe-cho, Kyoto, Japan 606-8501.*
E-mail: motoy@kuhp.kyoto-u.ac.jp

Received 6 April 2007; revised 3 August 2007; accepted 14 August 2007; published online 17 October 2007

Bone morphogenetic proteins (BMPs) are phylogenetically conserved signaling molecules that belong to the transforming growth factor-β superfamily.[1] Although these proteins were first identified by their capacity to promote endochondral bone formation, they are involved in the cascades of body patterning and morphogenesis. Furthermore, BMPs play important roles after birth in the pathophysiology of several diseases, including osteoporosis, arthritis, pulmonary hypertension, and kidney diseases.[2]

Bone morphogenetic protein-7 is a 35-kDa homodimeric protein, and kidney is the major site of BMP-7 synthesis during embryogenesis as well as in postnatal development. *BMP-7*-deficient mice die shortly after birth due to severe renal hypoplasia.[3,4] Mutant kidneys suffer gradual cessation of nephrogenesis, associated with a reduction in ureteric bud branching and loss of metanephric mesenchyme, indicating that BMP-7 is essential for survival and differentiation of mesenchymal cells in kidney development.[5] In postnatal life, many developmental features are recapitulated during renal injury, and BMP-7 has been shown to be important in both preservation of kidney function and resistance to injury. For example, BMP-7 inhibits tubular epithelial cell dedifferentiation,[6–10] mesenchyme transformation, and apoptosis stimulated by various renal injuries, and has an anti-inflammatory effect in models of both acute and chronic renal failure.[11]

The local activity of endogenous BMP-7 is controlled not only by the precise regulation of its expression, but also by certain classes of molecules that bind to BMP-7, acting as positive[12] or negative regulators of BMP-7 activity in the kidney.[2,13–15] BMP antagonists function through direct association with BMP, thus inhibiting the binding of BMP to its receptors, and define the boundaries of BMP activity.

Recently, we found that the product of uterine sensitization-associated gene-1 (USAG-1) acts as a kidney-specific BMP antagonist, and that USAG-1 binds to and inhibits the biological activity of BMP-7.[16] We further demonstrated that *USAG-1*-deficient mice are resistant to kidney injury, and that USAG-1 is the central negative regulator of BMP

function in the adult kidney.[17] Because the interaction between BMP-7 and USAG-1 seems to play critical roles in the kidney, we analyzed the balance between USAG-1 and BMP-7 expression in kidney injury and development, and demonstrated the reciprocal relationship between USAG-1 and BMP-7 expression in kidney injury and development. Close examination of USAG-1 expression in developing kidneys further provided a clue to proximal–distal differentiation mechanism of nephron by demonstrating the possibility that each single cell in an immature nephron controls its own fate to become proximal or distal tubule cell. In addition, USAG-1 expression in the kidney biopsy could be a powerful diagnostic tool to predict renal prognosis.

RESULTS

Generation of *USAG-1*$^{+/LacZ}$ knock-in mice

To facilitate the temporal and spatial analyses of USAG-1 expression, we generated in-frame *USAG-1*$^{+/LacZ}$ mice. In our previous work, the nuclear *lacZ* reporter gene that was knocked in[17] proved unsuitable for signal detection. In this work, the cytoplasmic *lacZ* reporter gene was used to replace the open reading frame of *USAG-1* and create a novel knock-in allele (Figure 1a). While *USAG-1*$^{+/LacZ}$ mice showed no overt defects, *USAG-1*$^{LacZ/LacZ}$ mice presented the same teeth phenotype as observed in the original *USAG-1* mutants.[17] *In situ* hybridization (ISH) of a *USAG-1* antisense probe to whole embryos at E9.5 and adult kidney specimen confirmed that lacZ staining in *USAG-1*$^{+/LacZ}$ mice reflected authentic *USAG-1* gene expression (Figure 1d).

USAG-1 is expressed in distal tubules and overlaps with BMP-7 in distal convoluted tubules

To further analyze the localization of USAG-1 expression in the kidney, we used several well-characterized segment markers. First, we clarified the segments in which well-known segment markers are expressed (Figure 2a). Tamm Horsfall glycoprotein (THP) was expressed in thick ascending limb. The calbindin D28K was expressed in distal convoluted tubules (DCTs) and connecting tubules (CTs). Using the antibody from Upstate, NaKATPase α-1 subunit was strongly expressed in thick ascending limb, DCT, and CT. AQP-1 was expressed in proximal tubules, descending thin limb, and possibly in ascending thin limb, while AQP-2 was expressed in the collecting ducts (CDs)[18] and CTs as reported.

Next, we analyzed the localization of USAG-1 in adult kidneys using these markers, and demonstrated that all the tubules expressing calbindin D28K or THP in the cortex expressed USAG-1 (Figure 2b and c). In the outer medulla, USAG-1 expression completely overlapped with THP (Figure 2d) and NaKATPase (Figure 2e), but not with AQP-2 (Figure 2f) or AQP-1 (Figure 2g). In addition, USAG-1 expression in the cortex did not overlap with AQP-2 (Figure 2f) or AQP-1 (Figure 2g), except for CTs, which were double positive for *lacZ* transcript and AQP-2 (data not shown). In the inner medulla, USAG-1 expression was not detected (Figure 1d). From these findings, we concluded that USAG-1 is predominantly expressed in the distal tubules, more specifically, in thick ascending limb, DCT, and CT in adult kidneys.

For comparison, the expression of BMP-7 was determined using *BMP-7*$^{+/LacZ}$ mice, and the tubules expressing calbindin D28K (Figure 2h) or AQP-2 (data not shown) were positive for *lacZ* transcript, indicating that BMP-7 is expressed in DCT, CT, and CD as previously reported (Figure 2a).[11]

USAG-1 emerges in developing nephrons and colocalizes with BMP-7 only in differentiated tubules

Next, we examined the expression of USAG-1 and BMP-7 in kidney development. The expression of USAG-1 increased toward the later stage of development, and peaked at E17.5, while BMP-7 was constantly expressed during kidney development and decreased at perinatal period (Figure 3a). As a result, the ratio between USAG-1 and BMP-7 expression increased significantly toward the later stage of development (Figure 3a). We also compared the ratio between other BMP antagonists and BMP-7, and demonstrated that USAG-1 is predominantly the major BMP antagonist during kidney development (Figure 3a). At E13.5, USAG-1 expression was almost absent (Figure 3b), while BMP-7 expression was intensely expressed in ureteric buds, adjacent metanephric mesenchyme, and part of comma-shaped body (Figure 3c). At E15.5, USAG-1 expression was still absent in the comma-shaped body, but was strongly detected in more differentiated tubular epithelial cells in the medulla, in a pattern similar to that of BMP-7, except for the expression in the podocyte layers of the developing glomeruli, where USAG-1 expression was absent (Figure 3b and c). Therefore, we conclude that USAG-1 emerges in developing nephrons and colocalizes with BMP-7 only in differentiated tubules (Figure 3d). We also examined the expression of several segmental markers in *USAG-1*-deficient kidney to determine whether the developmental process is modified; however, we could not observe any difference in the expression pattern of these markers (data not shown).

Mosaicism of proximal tubule marker-positive cell and distal tubule marker-positive cell in a single immature nephron

From E17.5 to the neonatal period, two patterns of USAG-1 expression were observed in the kidneys: a strong signal in distal tubules (Figure 3b, arrowheads) and a weak, patchy signal in the cortex (Figure 3b, arrows). To demonstrate that both signals were not due to endogenous β-galactosidase activity in the kidney, kidneys of wild-type mice were subjected to lacZ staining and incubated for the same period of time, but no signal was detected (Figure 3b).

We further analyzed the property of these signals with segment markers, and found that the strong signal in neonatal *USAG-1*$^{+/LacZ}$ kidneys colocalized with THP and NaKATPase (Figure 4a and b), but not with AQP-1 or AQP-2 (Figure 4c and d). Calbindin D28K was hardly detected in the

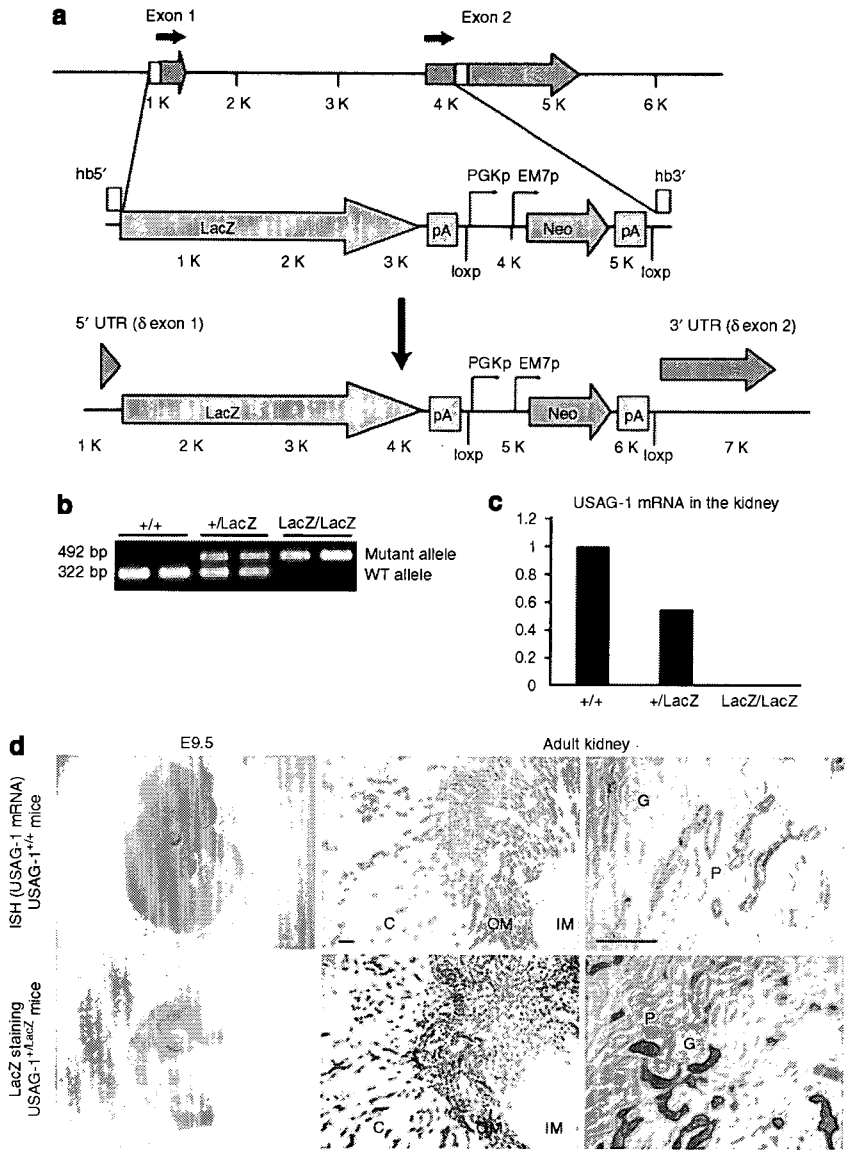

Figure 1 | Generation of USAG-1 $^{+/LacZ}$ knock-in mice by gene targeting. (**a**) Design of *Sostdc1* (gene symbol for *USAG-1*) null allele with concomitant replacement by LacZ. Light gray arrows depict the two exons; black arrows indicate the coding sequence. The homology boxes used for bacterial homologous recombination (BHR) are depicted as white (hb5′ and hb3′). The entire coding sequence of *Sostdc1* was replaced by LacZ/Neo, in a manner such that the initiating ATG of *Sostdc1* became the ATG of LacZ. The reporter open reading frame (ORF), LacZ, is followed by an SV40 polyadenylation signal and SV40-derived associated sequence[31] (purple boxes), whereas, the Neo ORF is followed by the mouse PGK polyadenylation signal and associated sequence[32] (yellow boxes). All of these elements are standard elements used by Velocigene.[29] The replacement afforded into the *Sostdc1* BAC by BHR is also translated in an identical manner into the mouse genome during targeting. Therefore, all the features shown above are also those present in the modified *Sostdc1* locus in the targeted embryonic stem (ES) cells. (**b**) PCR genotyping of *USAG-1* $^{+/+}$, *USAG-1* $^{+/LacZ}$, and *USAG-1* $^{LacZ/LacZ}$ littermates. (**c**) Real-time RT-PCR analysis of *USAG-1* mRNA in the kidneys of *USAG-1* $^{+/+}$, *USAG-1* $^{+/LacZ}$, and *USAG-1* $^{LacZ/LacZ}$ littermates. Expression of *USAG-1* was normalized to that of *GAPDH* and expressed relative to that in *USAG-1* $^{+/+}$ mice. (**d**) ISH of whole embryo and adult kidney section revealed a similar distribution of *USAG-1* mRNA and *lacZ* transcripts. C, cortex; OM, outer medulla; IM, inner medulla; P, proximal tubule; G, glomerulus. Bar = 100 μm.

immature nephron at this stage. On the other hand, only the weak, patchy signal, but not the strong signal, colocalized with the expression of the lectin-binding sites for Lotus Tetragonolobus Agglutnin (LTA) (Figure 4e), the marker for proximal tubules.[19] NDRG1, the cytoplasmic protein upregulated in several stress stimuli,[20] is known to be expressed in the proximal tubules and CDs in the kidney.[21] The weak, patchy signal of lacZ staining also colocalized with NDRG1 expression (Figure 4f), indicating that these tubules with weak, patchy signal of lacZ staining possess proximal tubule property, as well. AQP-1 was partially positive in the descending part of weak, patchy blue tubules (Figure 4d), possibly indicating that these tubules might have the characteristics of proximal tubules and thin limbs of Henle.

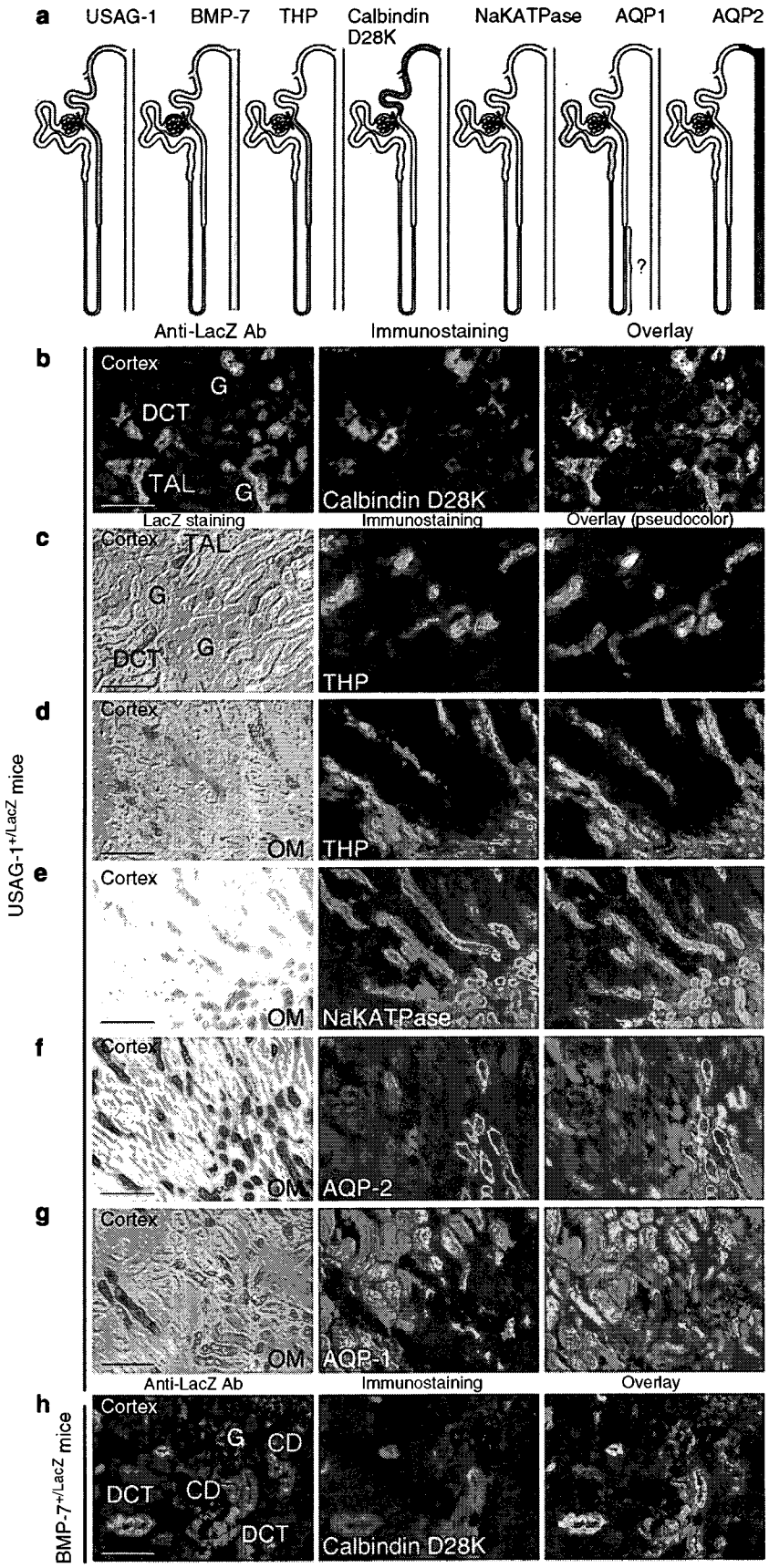
a
USAG-1
BMP-7
THP
Calbindin D28K
NaKATPase
AQP1
AQP2
?
Anti-LacZ Ab
Immunostaining
Overlay
b
Cortex
G
DCT
TAL
G
Calbindin D28K
LacZ staining
Immunostaining
Overlay (pseudocolor)
c
Cortex
TAL
G
DCT
G
THP
d
Cortex
OM
THP
e
Cortex
OM
NaKATPase
f
Cortex
OM
AQP-2
g
Cortex
OM
AQP-1
USAG-1+/LacZ mice
Anti-LacZ Ab
Immunostaining
Overlay
h
Cortex
G
CD
DCT
CD
DCT
Calbindin D28K
BMP-7+/LacZ mice

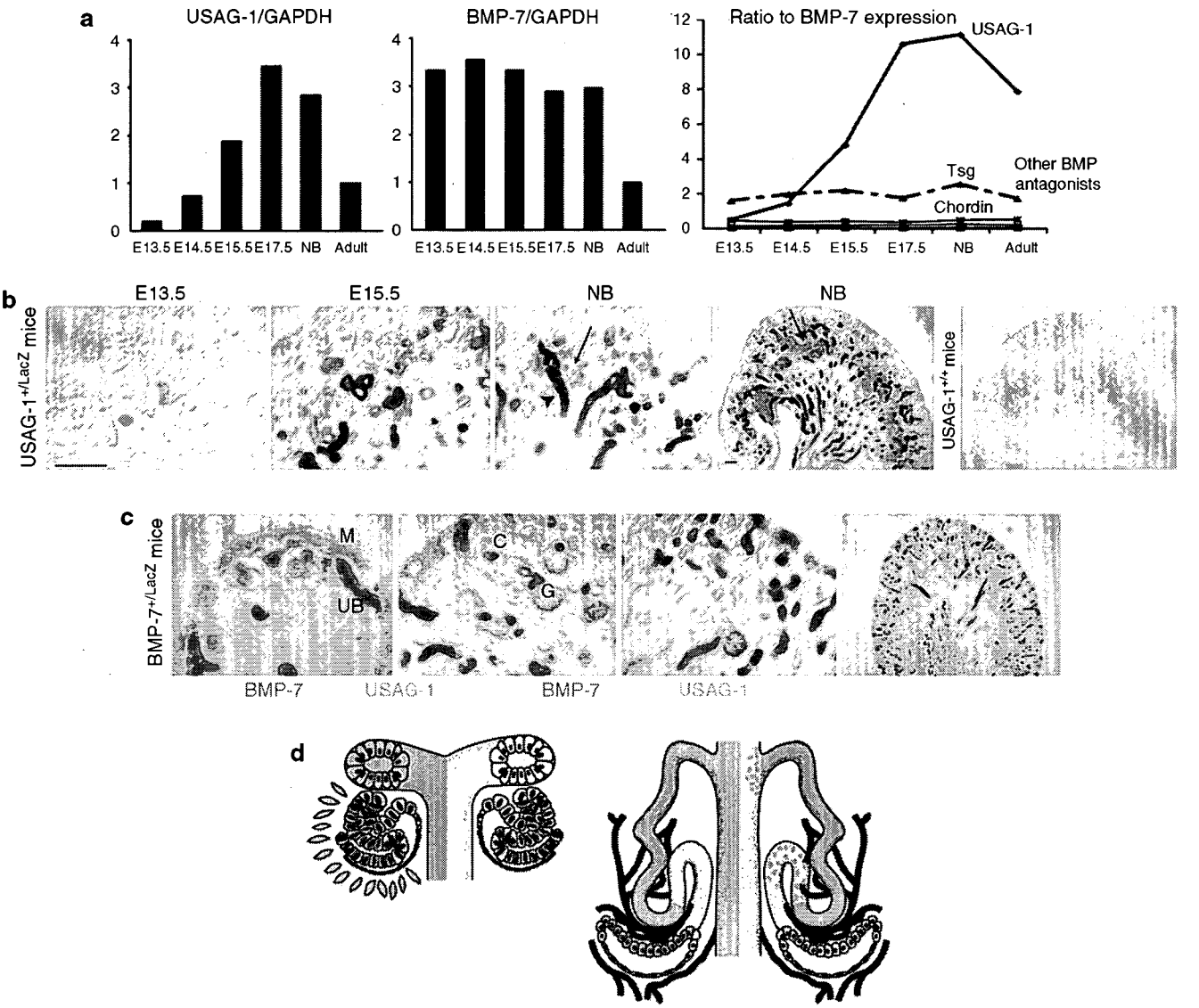

Figure 3 | USAG-1 emerged in developing nephrons and colocalized with BMP-7 in differentiated tubules. (**a**) Expression of USAG-1 and ratio of USAG-1/BMP-7 expression increased in kidney development. Metanephric kidneys from five to six embryos at indicated time points, and kidneys from seven neonates were collected and subjected to RNA extraction. Expression levels of USAG-1 and BMP-7 were normalized to the expression of GAPDH and expressed relative to the expression level in the adult kidney. The ratio of USAG-1 and other BMP antagonists to BMP-7 expression was determined as described (see Materials and Methods). (**b** and **c**) Localization of *lacZ* transcripts in developing *USAG-1*$^{+/LacZ}$ (**b**) and *BMP-7*$^{+/LacZ}$ (**c**) kidneys. Expression of *USAG-1/lacZ* transcripts did not emerge in immature nephrons, where BMP-7 facilitates differentiation, but was strong and overlapped with that of BMP-7 in the fully differentiated tubules (arrowheads). Besides, the strong signal of *USAG-1/lacZ* transcripts in distal tubules (arrowhead), a weak, patchy signal was observed in the neonatal kidneys (arrows). UB, ureteric bud; M, mesenchyme; C, comma-shaped body; G, glomerulus. Bar = 100 μm. (**d**) Schematic illustration demonstrating the expression of USAG-1 and BMP-7 during kidney development. USAG-1 expression was negative in the immature nephron, where BMP-7 was strongly expressed and promoted differentiation. USAG-1 expression emerged in more differentiated tubules and overlapped with that of BMP-7.

Figure 2 | USAG-1 and BMP-7 overlap in DCTs. (**a**) Schematic illustration demonstrating the expression of USAG-1, BMP-7, and other segment markers in the nephron. USAG-1 is expressed in thick ascending limb (TAL), DCTs, and in CTs, while BMP-7 is expressed in DCT, CT, and in CD. (**b**) Tubules positive for calbindin D28K are positive for *LacZ* transcripts in the kidneys of *USAG-1*$^{+/LacZ}$ mice. G, glomerulus. Bar = 100 μm. (**c**) Tubules positive for THP in the cortex are positive for *LacZ* transcripts in the kidneys of *USAG-1*$^{+/LacZ}$ mice. (**d**) Tubules positive for THP in the cortex and medulla are positive for *LacZ* transcripts in the kidneys of *USAG-1*$^{+/LacZ}$ mice. OM, outer medulla. (**e**) Tubules positive for NaKATPase in the cortex and medulla are positive for *LacZ* transcripts in the kidneys of *USAG-1*$^{+/LacZ}$ mice. (**f** and **g**) Tubules positive for AQP-2 (**f**) or AQP-1 (**g**) are negative for *LacZ* transcripts in the kidneys of *USAG-1*$^{+/LacZ}$ mice. (**h**) Tubules positive for calbindin D28K are positive for *LacZ* transcripts in the kidneys of *BMP-7*$^{+/LacZ}$ mice. *LacZ* transcripts in the kidneys of *BMP-7*$^{+/LacZ}$ mice are also positive in CD and podocyte in glomeruli.

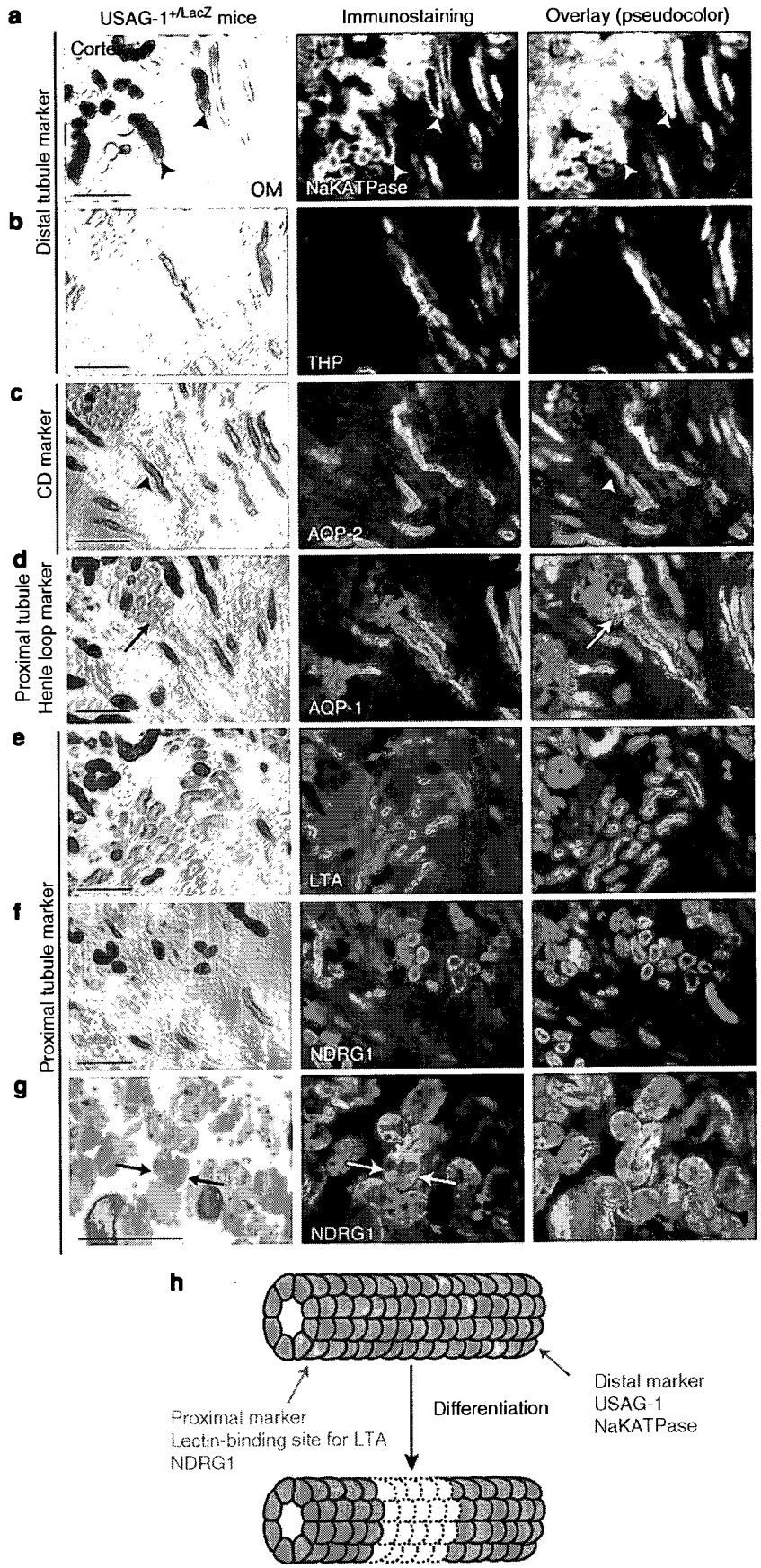
a
USAG-1+/LacZ mice
Immunostaining
Overlay (pseudocolor)
Cortex
OM
NaKATPase
Distal tubule marker
b
THP
c
CD marker
AQP-2
d
Proximal tubule
Henle loop marker
AQP-1
e
LTA
f
Proximal tubule marker
NDRG1
g
NDRG1
h
Proximal marker
Lectin-binding site for LTA
NDRG1
Differentiation
Distal marker
USAG-1
NaKATPase

Close examination of these tubules further clarified that the weak, patchy signal of lacZ staining and NDRG1 signals were not overlapping in a single cell, but were complementary in the single tubule (Figure 4g); therefore, the tubule in this area was made up of two types of epithelial cells: those with distal tubule property and those with proximal tubule property (Figure 4h). To exclude the possibility that lacZ staining quenches the fluorescence of other markers, immunostaining of the serial sections was performed and demonstrated similar results (data not shown).

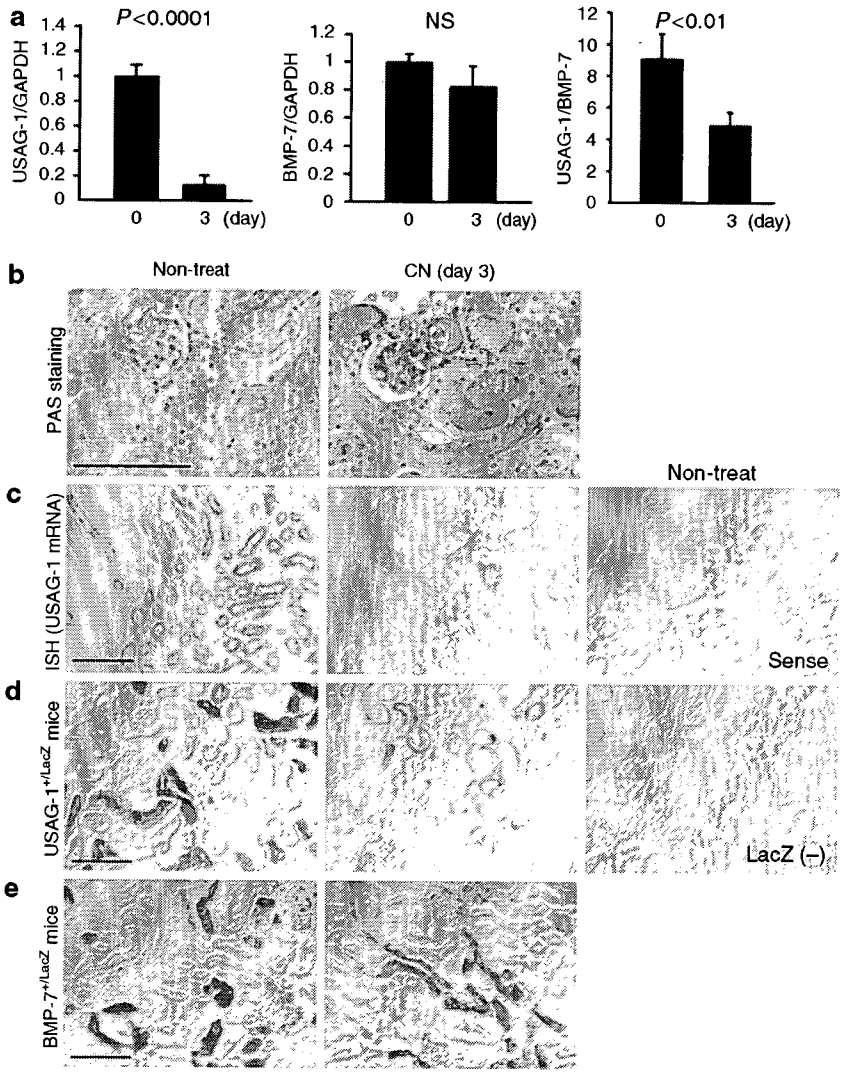

Figure 5 | Expression of USAG-1 decreased in tubular injury. (**a**) Expression of *USAG-1* mRNA decreased in acute tubular injury. Expression of USAG-1 and BMP-7 and the ratio between USAG-1 and BMP-7 expression during cisplatin nephrotoxicity (CN) were determined by real-time RT-PCR. Expression of USAG-1 and BMP-7 was normalized to that of GAPDH and expressed relative to that in mice on day 0. The ratio between USAG-1 and BMP-7 expression was determined by setting the standard curve with plasmids encoding each gene at various concentrations and analyzing the copy number of each gene contained in kidney cDNA (see Results). $N = 4$–6 for each experiment. (**b**–**e**) Representative histological findings (**b**), ISH of *USAG-1* mRNA (**c**), and lacZ staining of the *USAG-1*$^{+/LacZ}$ (**d**), and *BMP-7*$^{+/LacZ}$ (**e**) kidneys during CN. Bar = 100 μm.

Figure 4 | Mosaicism of proximal tubule marker-positive cell and distal tubule marker-positive cell in a single immature nephron. (**a**) Strong (arrowheads) and weak, patchy signal of *lacZ* transcripts in neonatal *USAG-1*$^{+/LacZ}$ kidneys colocalized with NaKATPase. Bar = 100 μm. (**b**) Strong signal of *lacZ* transcripts in neonatal *USAG-1*$^{+/LacZ}$ kidneys colocalized with THP. (**c**) *LacZ* transcripts in neonatal *USAG-1*$^{+/LacZ}$ kidneys did not colocalize with AQP-2. (**d**) AQP-1 was partially positive in the descending tubules with weak, patchy signal of *lacZ* transcripts (arrow). (**e**) Weak, patchy signal of *lacZ* transcripts colocalized with lectin-binding sites for Lotus Tetragonolobus Agglutnin (LTA). (**f**) Weak, patchy signal of *lacZ* transcripts colocalized with NDRG1. (**g**) Close examination of the overlapping areas demonstrated that the weak, patchy signal of *lacZ* transcripts (arrows) was not overlapping with NDRG1 expression, but was complementary in a single tubule. (**h**) Working hypothesis for proximal–distal differentiation mechanism of kidney tubules. Proximal tubule marker-positive cells (green) lie side by side with distal tubule marker-positive cells (red) in a single immature nephron. It is postulated that each single cell possesses its cell fate to become proximal or distal tubular cell.

The ratio between USAG-1 and BMP-7 expression was reduced in tubular injury and increased in tubular regeneration

We also examined the expression of USAG-1 and BMP-7 in kidney injury. Administration of cisplatin causes acute tubular necrosis and apoptosis, leading to deterioration of renal function. USAG-1 but not BMP-7 mRNA in the kidney decreased at day 3 of cisplatin nephrotoxicity (Figure 5a). ISH and lacZ staining demonstrated that USAG-1 expression was significantly reduced at day 3 of cisplatin nephrotoxicity, while the lacZ staining in *BMP-7*$^{+/LacZ}$ mice was maintained (Figure 5c–e). At day 0 of cisplatin nephrotoxicity, the expression level of USAG-1 was much higher than that of BMP-7, but at day 3, the ratio between USAG-1 and BMP-7 expression was significantly decreased, indicating that the reduction of USAG-1 expression was more prominent than that of BMP-7.

Next, we examined the expression of USAG-1 in the kidney regeneration. Administration of folic acid (FA) to mice causes intratubular crystallization, which results in dilatation and degeneration of tubules, leading to transient acute renal failure[22] (Figure 6a). In contrast to the cisplatin nephrotoxicity model, damaged tubular epithelial cells proliferate and regenerate after several days, and renal function returns to normal by day 14 (Figure 6a). Expression of USAG-1 in this model decreased during tubular epithelial damage (day 1), but increased markedly during proliferation and regeneration of tubular epithelial cells (days 7–10), and

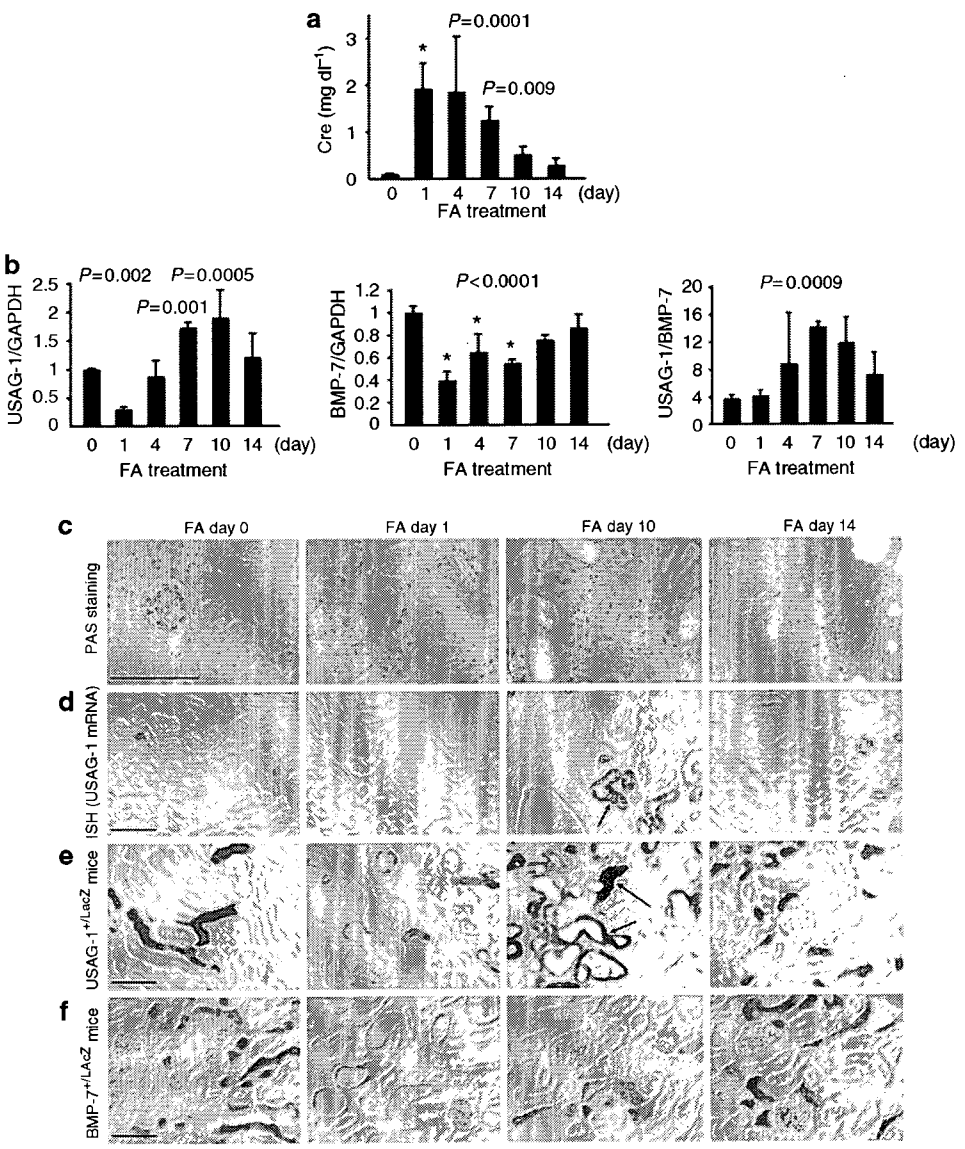

Figure 6 | Expression of USAG-1 increased in tubular regeneration. (**a**) Time course of serum creatinine level in FA nephrotoxicity model. (**b**) Expression of USAG-1 and BMP-7 and the ratio between USAG-1 and BMP-7 expression after FA treatment. $N = 4$–6 for each experiment. (**c**–**f**) Representative histological findings (**c**), ISH of USAG-1 mRNA (**d**), and lacZ staining of the *USAG-1*$^{+/LacZ}$ (**e**) and *BMP-7*$^{+/LacZ}$ kidneys (**f**) after FA treatment. Bar = 100 μm. USAG-1 was strongly detected in the irregularly lined regenerating epithelial cells (**d** and **e**; arrows).

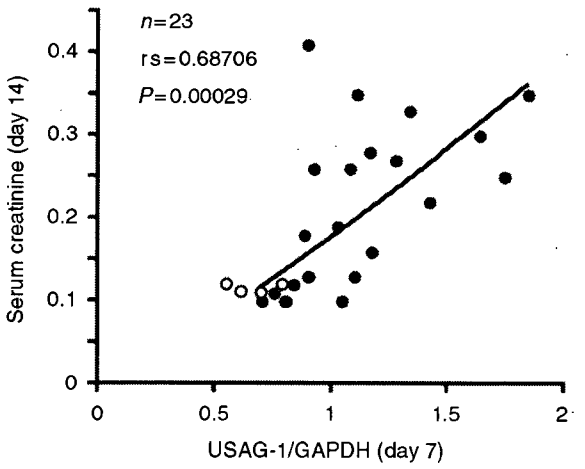

Figure 7 | USAG-1 as a diagnostic marker for renal prognosis. A significant correlation is observed between *USAG-1* expression in kidney biopsy sample at day 7 and serum creatinine at day 14 in FA nephrotoxicity (closed circle, $N = 23$). Open circles indicate control kidneys without FA nephrotoxicity ($N = 4$).

returned to the basal level when redifferentiation of tubular epithelial cells was completed (day 14), while the expression of BMP-7 increased gradually after the initial dip at day 1 (Figure 6b). ISH and lacZ staining demonstrated that USAG-1 was strongly detected in the irregularly lined regenerating tubular epithelial cells at day 10 (Figure 6d and e, arrows), which might account for the increase in USAG-1 expression at this time point (Figure 6b). The ratio between USAG-1 and BMP-7 expression was significantly increased during the regeneration phase (Figure 6b). We also compared the ratio between other BMP antagonists and BMP-7 in both kidney disease models, and demonstrated that USAG-1 is predominantly the major BMP antagonist during kidney injury (Figure S1).

USAG-1 as a predictive marker for renal prognosis

Because USAG-1 is a negative regulator of the renoprotective action of BMP-7, we postulated that high expression of USAG-1 in the kidney biopsy might predict poor renal prognosis.

Because regenerating tubules and damaged tubules are observed in the regenerating period (days 7–10) of FA nephrotoxicity and might mimic the situation in the clinical kidney biopsy specimen, we utilized the model and performed kidney biopsy at day 7 and examined renal function at day 14. Interestingly, the expression of USAG-1 in kidney biopsy at day 7 correlated significantly with renal function at day 14 (Figure 7), indicating the possibility that USAG-1 could be a predictive marker of renal prognosis. We also performed renal biopsies at days 1 and 10. As shown in Figure S2, USAG-1 expression at day 10 ($N = 4$, regenerating period) correlated well with future renal function at day 14, while USAG-1 expression at day 1 ($N = 8$, tubular damage period) did not. Therefore, we conclude that USAG-1 expression correlated well with future renal function when tubular regeneration is observed.

DISCUSSION

USAG-1 colocalizes with BMP-7 only in differentiated tubules in developing kidney

During kidney development, BMP-7, made by both metanephric mesenchyme and tubular epithelial cells (Figure 3c), is a facilitator of ureteric bud branching at low concentrations, but an inhibitor of branching at high concentrations.[23] The discrepancy is a part of a feedback mechanism that allows ureteric buds to branch into 'unpopulated' areas of mesenchyme, but not into areas already populated by nephrons and other bud branches. USAG-1 expression did not emerge in immature nephrons where BMP-7 facilitates differentiation, but was strongly expressed and overlapped with BMP-7 in fully differentiated tubules (Figure 3b and c). We also demonstrated that USAG-1 expression is lower than that of BMP-7 at E13.5, is comparable at E14.5 and E15.5, and is much higher at E17.5 and in newborns (Figure 3a). In addition, USAG-1 is the major BMP antagonist during kidney development (Figure 3a). These data support the idea that USAG-1 might function as a feedback mechanism for BMP-7 activity during kidney development. However, no developmental abnormality was observed in the kidney of *USAG-1*-deficient mice,[17] and some redundant factor might overcome the lack of USAG-1 in the kidney of *USAG-1*-deficient mice during development. Twisted gastrulation is one candidate for the redundancy, because the expression pattern is similar to that of USAG-1 and the expression level is the second highest among BMP antagonists to USAG-1 (Figure 3a).

USAG-1 expression gives an insight into proximal–distal differentiation mechanism of immature nephron

In spite of that USAG-1 expression was confined to distal tubules in adult kidney, weak, patchy expression of USAG-1 in neonatal kidneys colocalized with proximal tubular markers, such as lectin-binding site for Lotus Tetragonolobus and NDRG1 in the cortex. NaKATPase, another distal tubule marker, also colocalized with proximal tubular markers in the area (data not shown). AQP-1 was partially positive in the descending part of weak, patchy blue tubules, possibly indicating that these tubules might also have the property of proximal tubules and thin limbs of Henle. Close examination of the area double positive for proximal and distal markers further demonstrated that each single cell is not double positive for these two markers, but two types of cells positive for each marker intermingled with each other in a single tubule (Figure 4g and h). Little is known about the mechanism how uniform mesenchymal cells differentiate to a variety of cells, including glomerular epithelial cells, proximal tubular cells, and distal tubular cells, along the proximal–distal axis.[24] There has been a controversy between the following two hypotheses: gradient of growth factors brings the proximal–distal differentiation, or cell fate is determined for each cell. Recent studies revealed critical roles of Notch in the determination of proximal tubule cells and the fates of podocytes.[25–27] Our data might support the cell fate

hypothesis because the proximal tubule marker-positive cell lies side by side with the distal tubule marker-positive cell in a single tubule (Figure 4g and h), and such chimeric tubule could not be made by the gradient of growth factors. From these findings, we postulate that each single cell possesses its cell fate to become proximal tubular cell or distal tubular cell. Further study is needed to clarify how these chimeric tubules differentiate to mature tubules (Figure 4h). Interestingly, all tubule epithelial cells positive for proximal tubule marker reside in the chimeric tubules in neonatal kidney, while some distal tubule marker-positive cells reside outside the area and are terminally differentiated (Figure 4a and c, arrowheads, H), indicating the possible sequence of differentiation.

USAG-1 expression decreases in tubular injury and increases in tubular regeneration

In the adult kidney, we demonstrated that the expression of USAG-1 colocalized with BMP-7 in DCTs (Figure 2a) and decreased in acute tubular injury (Figure 5). The reduction of USAG-1 expression in renal injury is not simply due to loss of tubular epithelial cells, because USAG-1 expression decreased rapidly in the very early stage of diseases, when morphological changes of tubular epithelial cells were not obvious (data not shown).

During the recovery from renal failure, regeneration of tubular epithelial cells occurs via proliferation and redifferentiation of surviving renal cells.[28] In the FA model, USAG-1 expression decreased during tubular injury, increased markedly during the regeneration of surviving cells, and returned to the basal level after redifferentiation was completed (Figure 6b). In contrast, the expression of BMP-7 increased gradually to the basal level after the initial dip during tubular injury (Figure 6b), resulting in a significant increase in the ratio between USAG-1 and BMP-7 during regeneration. Further examination with *USAG-1*-deficient mice is needed to clarify the role of USAG-1 in the regeneration of kidney injury.

USAG-1 could be a diagnostic marker for renal prognosis

In the clinical setting, prediction of renal prognosis is difficult even with histological examination, because damaged tubules and regenerating tubules are mixed in the single specimen, and are indistinguishable by morphology. Because USAG-1 is a negative regulator of the renoprotective action of BMP-7, we postulated that high expression of USAG-1 during kidney diseases might be a sign of poor renal prognosis. Because the coexistence of regenerating tubules and damaged tubules in FA nephrotoxicity model resembles the situation of renal biopsy in patients, we utilized the model and proved that high expression of USAG-1 in kidney biopsy in regenerating period correlated well with poor renal prognosis. Because the expression of USAG-1 is confined to the kidney, serum concentration of USAG-1 might reflect the renal expression level of USAG-1. In that case, blood test for USAG-1 concentration might be enough to predict renal prognosis and is suitable for health examination.

MATERIALS AND METHODS

Derivation of USAG-1/LacZ mice

To generate a null allele of *Sostdc1* (gene symbol for *USAG-1*), the coding sequence was replaced with the coding sequence of the marker gene LacZ, using Velocigene technology, essentially as described (Figure 1a).[29] PCR genotyping was performed in all subsequent studies to allow specific detection of the genotype (Figure 1b). The sequences of the primers used were as follows: primer A, CCTTCTCTGTGTTTTCACTCCG; primer B, TGATTCAGGGTGCTG TTGC; and lacZRev, CCGTAATGGGATAGGTCACG.

β-gal staining and *in situ* hybridization

β-gal staining and ISH were performed as described previously.[17,29] Probe for ISH was designed to contain the open reading frame with the following length and GC content: USAG-1, 1.0 kbp (GC 52.6%). Hybridization was detected using an anti-DIG AP conjugate (Roche, Basel, Switzerland) and NBT/BCIP solution (Roche).

Histological studies and immunostaining

The kidneys were fixed in Carnoy's solution, embedded in paraffin, and sections (4 μm thick) were stained with periodic acid-Schiff for routine histological examination. Frozen sections of the kidneys and primary kidney tubular cells were immunostained as previously described.[30] Reagents utilized were anti-NaKATPase α-1 antibody (Ab) (Upstate, Billerica, MA, USA), anti-calbindin D28K (Sigma, St Louis, MO, USA), anti-Tamm Horsfall Protein Ab (Biomedical Technologies Inc.), anti-aquaporin 1 Ab (Chemicon, Temecula, CA, USA), anti-aquaporin 2 Ab (Calbiochem, Darmstadt, Germany), FITC-conjugated lotus tetragonolobus agglutinin (LTA) (Sigma), anti-LacZ Ab (Cappel, Solon, OH, USA), and anti-NDRG1 Ab.[20] For double staining, immunostaining was performed before β-gal staining, to avoid the possibility that the deposition of X-gal interferes with antibody binding to the antigen.

Quantification of mRNA by real-time RT-PCR

Real-time reverse transcription (RT)-PCR was performed as described previously.[17] Specific primers were designed using Primer Express software (Applied Biosystems, Foster City, CA, USA). To compare the expression levels of different genes, we used modified real-time PCR by setting the standard curves with plasmids encoding each gene at various concentrations, and analyzed the copy number of each gene contained in kidney cDNA as previously described.[17] Serially diluted cDNA or plasmids were used to generate the standard curve for each primer, and the PCR conditions were as follows: 50 °C for 2 min, 95 °C for 10 min, then 95 °C for 15 s, and 60 °C for 1 min for 40 cycles.

Kidney disease models

Cisplatin nephrotoxicity was caused as described previously.[17] Briefly, cisplatin (20 mg kg^{-1}, Sigma-Aldrich) was administered by a single intraperitoneal injection to 8-week-old female C57BL/6J mice (SLC Japan, Shizuoka, Japan). FA nephrotoxicity was caused by a single intraperitoneal injection of FA (250 mg kg^{-1}, Sigma-Aldrich) in 0.15 M $NaHCO_3$ to 11-week-old male C57BL/6J mice. The kidneys were collected at days 0, 1, 4, 10, and 14, with at least three animals at each time point.

Animal use

All mice were housed in specific pathogen-free conditions. All animal experiments were performed in accordance with the institutional guidelines as well as the National Institutes of Health (NIH) guidelines.

Statistical analysis

All assays were performed in triplicate. Data were presented as mean $\pm$ s.d. Statistical significance was assessed by analysis of variance, followed by Fisher's protected LSD *post hoc* test. Correlation was determined by Spearman's correlation analysis.

ACKNOWLEDGMENTS

We thank Drs Y Nabeshima, E Nishi, and T Nakamura for valuable comments and discussion; S Tahara and A Yoshioka for experiments not included in the manuscript; and A Hosotani for technical assistance. This study was supported by grants-in-aid from the Ministry of Education, Culture, Science, Sports, and Technology of Japan (177090551); a Center of Excellence grant from the Ministry of Education, Culture, Science, Sports, and Technology of Japan; a research grant for health sciences from the Japanese Ministry of Health, Labor and Welfare; a grant from the Astellas Foundation for Research on Metabolic Disorders; a grant from the Novartis Foundation for the promotion of science; a grant from Kato Memorial Trust for Nambyo Research; a grant from Hayashi Memorial Foundation for Female Natural Scientists; and a grant from Japan Foundation for Applied Enzymology.

SUPPLEMENTARY MATERIAL

Figure S1. Relative expression of USAG-1 and other BMP antagonists to BMP-7 in kidney disease models.

Figure S2. Significant correlation was observed between *USAG-1* expression and future serum creatinine (day 14) in case that kidney biopsy was performed at day 10 but not at day 1 in folic acid nephrotoxicity (closed circles).

REFERENCES

1. Reddi AH. Bone morphogenetic proteins and skeletal development: the kidney-bone connection. *Pediatr Nephrol* 2000; **14**: 598–601.
2. Massague J, Chen YG. Controlling TGF-beta signaling. *Genes Dev* 2000; **14**: 627–644.
3. Dudley AT, Lyons KM, Robertson EJ. A requirement for bone morphogenetic protein-7 during development of the mammalian kidney and eye. *Genes Dev* 1995; **9**: 2795–2807.
4. Luo G, Hofmann C, Bronckers AL *et al.* BMP-7 is an inducer of nephrogenesis, and is also required for eye development and skeletal patterning. *Genes Dev* 1995; **9**: 2808–2820.
5. Dudley AT, Robertson EJ. Overlapping expression domains of bone morphogenetic protein family members potentially account for limited tissue defects in BMP7 deficient embryos. *Dev Dyn* 1997; **208**: 349–362.
6. Kalluri R, Neilson EG. Epithelial–mesenchymal transition and its implications for fibrosis. *J Clin Invest* 2003; **112**: 1776–1784.
7. Zeisberg M, Hanai J, Sugimoto H *et al.* BMP-7 counteracts TGF-beta1-induced epithelial-to-mesenchymal transition and reverses chronic renal injury. *Nat Med* 2003; **9**: 964–968.
8. Zeisberg M, Shah AA, Kalluri R. Bone morphogenic protein-7 induces mesenchymal to epithelial transition in adult renal fibroblasts and facilitates regeneration of injured kidney. *J Biol Chem* 2005; **280**: 8094–8100.
9. Wang S, Chen Q, Simon TC *et al.* Bone morphogenic protein-7 (BMP-7), a novel therapy for diabetic nephropathy. *Kidney Int* 2003; **63**: 2037–2049.
10. Wang S, de Caestecker M, Kopp J *et al.* Renal bone morphogenetic protein-7 protects against diabetic nephropathy. *J Am Soc Nephrol* 2006; **17**: 2504–2512.
11. Gould SE, Day M, Jones SS *et al.* BMP-7 regulates chemokine, cytokine, and hemodynamic gene expression in proximal tubule cells. *Kidney Int* 2002; **61**: 51–60.
12. Lin J, Patel SR, Cheng X *et al.* Kielin/chordin-like protein, a novel enhancer of BMP signaling, attenuates renal fibrotic disease. *Nat Med* 2005; **11**: 387–393.
13. Reddi AH. Interplay between bone morphogenetic proteins and cognate binding proteins in bone and cartilage development: noggin, chordin and DAN. *Arthritis Res* 2001; **3**: 1–5.
14. Yanagita M. BMP antagonists: their roles in development and involvement in pathophysiology. *Cytokine Growth Factor Rev* 2005; **16**: 309–317.
15. Yanagita M. Modulator of bone morphogenetic protein activity in the progression of kidney diseases. *Kidney Int* 2006; **70**: 989–993.
16. Yanagita M, Oka M, Watabe T *et al.* USAG-1: a bone morphogenetic protein antagonist abundantly expressed in the kidney. *Biochem Biophys Res Commun* 2004; **316**: 490–500.
17. Yanagita M, Okuda T, Endo S *et al.* Uterine sensitization-associated gene-1 (USAG-1), a novel BMP antagonist expressed in the kidney, accelerates tubular injury. *J Clin Invest* 2006; **116**: 70–79.
18. Sasaki S, Fushimi K, Saito H *et al.* Cloning, characterization, and chromosomal mapping of human aquaporin of collecting duct. *J Clin Invest* 1994; **93**: 1250–1256.
19. Cho EA, Patterson LT, Brookhiser WT *et al.* Differential expression and function of cadherin-6 during renal epithelium development. *Development* 1998; **125**: 803–812.
20. Okuda T, Higashi Y, Kokame K *et al.* Ndrg1-deficient mice exhibit a progressive demyelinating disorder of peripheral nerves. *Mol Cell Biol* 2004; **24**: 3949–3956.
21. Wakisaka Y, Furuta A, Masuda K *et al.* Cellular distribution of NDRG1 protein in the rat kidney and brain during normal postnatal development. *J Histochem Cytochem* 2003; **51**: 1515–1525.
22. Long DA, Woolf AS, Suda T *et al.* Increased renal angiopoietin-1 expression in folic acid-induced nephrotoxicity in mice. *J Am Soc Nephrol* 2001; **12**: 2721–2731.
23. Gupta IR, Piscione TD, Grisaru S *et al.* Protein kinase A is a negative regulator of renal branching morphogenesis and modulates inhibitory and stimulatory bone morphogenetic proteins. *J Biol Chem* 1999; **274**: 26305–26314.
24. Dressler GR. The cellular basis of kidney development. *Annu Rev Cell Dev Biol* 2006; **22**: 509–529.
25. Cheng HT, Kopan R. The role of Notch signaling in specification of podocyte and proximal tubules within the developing mouse kidney. *Kidney Int* 2005; **68**: 1951–1952.
26. Chen L, Al-Awqati Q. Segmental expression of Notch and Hairy genes in nephrogenesis. *Am J Physiol Renal Physiol* 2005; **288**: F939–F952.
27. McLaughlin KA, Rones MS, Mercola M. Notch regulates cell fate in the developing pronephros. *Dev Biol* 2000; **227**: 567–580.
28. Thadhani R, Pascual M, Bonventre JV. Acute renal failure. *N Engl J Med* 1996; **334**: 1448–1460.
29. Valenzuela DM, Murphy AJ, Frendewey D *et al.* High-throughput engineering of the mouse genome coupled with high-resolution expression analysis. *Nat Biotechnol* 2003; **21**: 652–659.
30. Yanagita M, Arai H, Ishii K *et al.* Gas6 regulates mesangial cell proliferation through Axl in experimental glomerulonephritis. *Am J Pathol* 2001; **158**: 1423–1432.
31. Thimmappaya B, Zain BS, Dhar R *et al.* Nucleotide sequence of DNA template for the 3′ ends of SV40 mRNA. II. The sequence of the DNA fragment *Eco*RII-F and a part of *Eco*RII-H. *J Biol Chem* 1978; **253**: 1613–1618.
32. Adra CN, Boer PH, McBurney MW. Cloning and expression of the mouse pgk-1 gene and the nucleotide sequence of its promoter. *Gene* 1987; **60**: 65–74.

Modulator of bone morphogenetic protein activity in the progression of kidney diseases

M Yanagita[1]

[1]*COE Formation for Genomic Analysis of Disease Model Animals with Multiple Genetic Alterations, Graduate School of Medicine, Kyoto University, Kyoto, Japan*

Tubular damage and interstitial fibrosis is a final common pathway leading to end-stage renal disease, and once tubular damage is established, it cannot be reversed by currently available treatment. The administration of bone morphogenetic protein-7 (BMP-7) in pharmacological doses repairs established tubular damages and improves renal function in several kidney disease models; however, pathophysiological role of endogenous BMP-7 and regulatory mechanism of its activities remain elusive. The activity of BMP is precisely regulated by certain classes of molecules termed BMP agonist/antagonist. In this review, roles of BMP agonist/antagonists possibly modulating the activity of BMP in kidney diseases are discussed. Our group demonstrated that uterine sensitization-associated gene-1 (USAG-1), a novel BMP antagonist abundantly expressed in the kidney, is the central negative regulator of BMP-7 in the kidney, and that mice lacking USAG-1 (*USAG-1*$^{-/-}$ mice) are resistant to kidney injuries. *USAG-1*$^{-/-}$ mice exhibited markedly prolonged survival and preserved renal function in acute and chronic renal injuries. Renal BMP signaling, assessed by phosphorylation of Smad proteins, is significantly enhanced in *USAG-1*$^{-/-}$ mice during renal injury, indicating that the preservation of renal function is attributed to enhancement of endogenous BMP-7 signaling. Furthermore, the administration of neutralizing antibody against BMP-7 abolished renoprotection in *USAG-1*$^{-/-}$ mice, indicating that USAG-1 plays a critical role in the modulation of renoprotective action of BMP, and that inhibition of USAG-1 will be promising means of development of novel treatment for kidney diseases.

Kidney International (2006) **70,** 989–993. doi:10.1038/sj.ki.5001731; published online 26 July 2006

KEYWORDS: BMP-7; ectodin; wise; gremlin; KCP; kidney diseases

Correspondence: *M Yanagita, COE Formation for Genomic Analysis of Disease Model Animals with Multiple Genetic Alterations, Graduate School of Medicine, Kyoto University, Kyoto 606-8507, Japan.*
E-mail: motoy@kuhp.kyoto-u.ac.jp

Received 11 March 2006; revised 13 May 2006; accepted 2 June 2006; published online 26 July 2006

BMP-7 IN KIDNEY DISEASES

Bone morphogenetic proteins (BMPs) are phylogenetically conserved signaling molecules that belong to the transforming growth factor-β superfamily. Although these proteins were first identified by their capacity to promote endochondral bone formation, they are involved in the cascades of body patterning and morphogenesis. Furthermore, BMPs play important roles after birth in the pathophysiology of several diseases, including osteoporosis, arthritis, pulmonary hypertension, cerebrovascular diseases, and cancer and kidney diseases.

BMP-7, also known as osteogenic protein-1, is a 35-kDa homodimeric protein, and kidney is the major site of BMP-7 synthesis during embryogenesis as well as postnatal development.[1] Its genetic deletion in mice leads to severe impairment of kidney development, resulting in perinatal death.[2,3] Expression of BMP-7 in adult kidney is confined to distal collecting tubules and podocytes of glomeruli,[4] and the expression decreases in several kidney disease models, including acute ischemic renal injury, tubulointerstitial fibrosis, diabetic nephropathy, and remnant kidney model.[5] Recently, several reports indicate that the administration of pharmacological doses of BMP-7 inhibits and repairs acute and chronic renal injury in animal models.[6–8] The administration of BMP-7 reverses transforming growth factor-β1-induced fibrogenesis and epithelial-to-mesenchymal transition (EMT) and induces mesenchymal-to-epithelial transition *in vitro*,[8] inhibits the induction of inflammatory cytokine expression,[4] attenuates inflammatory cell infiltration, and reduces apoptosis of tubular epithelial cells in renal disease models. Collectively, BMP-7 plays critical roles in repairing processes of the renal tubular damage in kidney diseases. However, the physiological role and precise regulatory mechanism of endogenous BMP-7 activity remain elusive.

REGULATORY MECHANISM OF BMP ACTIVITY

The local activity of endogenous BMP is controlled by at least three different mechanisms. First, the expression pattern of BMP and its cell surface receptors controls local activity of BMP. Second, high-affinity binding of BMP to extracellular matrix increases its local concentration. Vukicevic *et al.*[9] previously showed that BMP-7 binds to basement membrane

components including type IV collagen. In addition, Gregory *et al.*[10] recently demonstrated that the prodomain of BMP-7 targets BMP-7 complex to the extracellular matrix. In most tissues, *bmp* mRNA expression and BMP protein are found colocalized.[9] Restricted diffusion of BMP proteins should increase its local concentration.

Finally, BMP signaling is precisely regulated by certain classes of molecules termed as BMP antagonists.[11] BMP antagonists function through direct association with BMPs, thus prohibiting BMPs from binding their cognate receptors. The interplay between BMP and their antagonists fine-tunes the level of available BMPs, and governs developmental and cellular processes as diverse as establishment of the embryonic dorsal–ventral axis, induction of neural tissue, formation of joints in the skeletal system, and neurogenesis in the adult brain. The indispensable roles of BMP-7 in the kidney led us to postulate the existence of some BMP antagonist that modulates the activities of BMP-7 in the kidney.

GREMLIN: BMP ANTAGONIST WITH A ROLE IN KIDNEY DEVELOPMENT

Gremlin was identified from a *Xenopus* ovarian library for activities inducing secondary axis, and it encodes 28-kDa protein that binds to BMP-2/4 and inhibits their binding to the receptors.

Gremlin knockout mice are neonatally lethal because of the lack of kidneys and septation defects in the lung. Gremlin is expressed in metanephric mesenchyme surrounding ureter tips, and gremlin-mediated BMP antagonism is essential to induce metanephric kidney development.[12]

Gremlin is also known as IHG-2 (induced in high glucose 2) because its expression in cultured kidney mesangial cells is induced by high ambient glucose, mechanical strain, and transforming growth factor-β.[13] The expression of gremlin in adult kidney is almost undetectable in healthy status, but the expression increases in several kidney disease models, including diabetic nephropathy,[13] cisplatin nephrotoxicity,[14] and unilateral ureteral obstruction. However, the role of gremlin in the progression of kidney diseases remained to be elucidated.

NOGGIN

Noggin is a 32 kDa glycoprotein secreted by Spemann organizer of *Xenopus* embryos, and is found to rescue dorsal development in the ultraviolet-induced ventralized embryos. Noggin binds to BMP-2 and BMP-4 with high affinity and to BMP-7 with low affinity, and prevent BMPs from binding to its receptors. In mice, noggin is expressed in the node, notochord, dorsal somite, condensing cartilage, and immature chondrocytes, and is essential in skeletal and joint development.

Recently, it is reported that overexpression of noggin in podocytes leads to the development of mesangial expansion, indicating the importance of endogenous BMP signaling in the maintenance of glomerular structure. Because the expression of noggin is almost undetectable in healthy and diseased kidney, other negative regulator of endogenous BMP might play a role in glomerular mesangial expansion.

USAG-1 AS A NEGATIVE REGULATOR OF BMP IN THE KIDNEY

Discovery and characterization of USAG-1

Through a genome-wide search for kidney-specific transcripts, our group found a novel gene, which encodes a secretory protein with a signal peptide and cysteine-rich domain.[15] The rat ortholog of the gene was previously reported as a gene of unknown function that was preferentially expressed in sensitized endometrium of rat uterus, termed uterine sensitization-associated gene-1 (USAG-1). Amino-acid sequences encoded in rat and mouse cDNAs are 97 and 98% identical to the human sequence, respectively, indicating high degrees of sequence conservation.

Domain search predicted this protein to be a member of the cystine-knot superfamily, which comprises of growth factors, BMPs, and BMP antagonists. Homology search revealed that USAG-1 has significant amino-acid identities (38%) to sclerostin, the product of the *SOST* gene. Mutations of *SOST* are found in patients with sclerosteosis, a syndrome of sclerosing skeletal dysplasia. Because sclerostin was subsequently shown to be a new member of BMP antagonist expressed in bones and cartilages, USAG-1 is postulated to be a BMP antagonist expressed in the kidney.

USAG-1 protein is a 28–30 kDa secretory protein and behaves as a monomer, in spite that a number of BMP antagonists form disulfide-bridged dimers.[15,16] This is consistent with the fact that USAG-1 protein does not have the extra cysteine residues present in noggin and differential screening-selected gene aberrative in neuroblastoma (DAN), which are necessary to make inter-molecular disulfide bridges. Recombinant USAG-1 protein physically interacts with BMP-2, -4, -6, and -7, leading to the inhibition of alkaline phosphatase activities induced by each BMP in C2C12 cells and MC3T3-E1 cells dose-dependently,[15,16] whereas sclerostin only inhibits BMP-6 and BMP-7 activities.

Furthermore, the activity of USAG-1 as a BMP modulator was confirmed *in vivo* using *Xenopus* embryogenesis. Injection of synthetic RNA encoding BMP antagonists to the ventral portion of *Xenopus* embryos inhibits the ventralizing signal of endogenous BMP, and induces dorsalizing phenotypes of the embryos, including secondary axis formation and hyperdorsalization. The injection of as little as 100 pg USAG-1 mRNA was sufficient to cause secondary axis formation, and injection of increasing doses of mRNA up to 1000 pg led to a corresponding increase in the frequency of dorsalization phenotypes, whereas embryos developed normally when irrelevant mRNA was injected.

Expression of USAG-1

In mouse embryogenesis, expression of USAG-1 mRNA was first detected on E11.5 and increased toward E17.5.[15] *In situ* hybridization of mouse embryos on E11.5 revealed moderate expression of USAG-1 mRNA in branchial arches and